The temperature dependence of the forbidden-hyperfine spectrum of rare earth S-state ions in cubic crystals
by Don Kay Worsencroft

A thesis submitted to the Graduate Faculty in partial fulfillment of the requirements for the degree of DOCTOR OF PHILOSOPHY in Physics
Montana State University

Abstract:
The temperature dependence of the intensities of the electron paramagnetic resonance (E.P.R..) spectrum for one percent Eu++ impurities in fluorite crystals has been investigated. This temperature dependence has been analyzed and has been shown to result from crystal expansion due to anharmonic terms of the lattice vibrations and from the harmonic terms which modulate the crystal-field as seen by the paramagnetic electrons.

It was determined that the relative intensities between forbidden and allowed hyperfine lines varied with temperature as [formula not captured by OCR] Good agreement between the predicted temperature dependence and the experiment were found; however, the value of C based on point charge calculations was subject to some question because of crystal-field parameter values.

In the analysis of the hyperfine spectrum as it depends on spatial orientation with respect to the magnetic field, certain "forbidden" hyperfine lines, heretofore not identified, were cataloged.

THE TEMPERATURE DEPENDENCE OF THE FORBIDDEN-HYPERFINE SPECTRUM OF RARE EARTH S-STATE IONS IN CUBIC CRYSTALS

by

DON KAY WORSENCROFT

A thesis submitted to the Graduate Faculty in partial fulfillment of the requirements for the degree

of

DOCTOR OF PHILOSOPHY

in

Physics

Approved:

Head, Major Department

Chairman, Examining Committee

Graduate Dean

MONTANA STATE UNIVERSITY
Bozeman, Montana

August, 1970

ACKNOWLEDGEMENTS

The author wishes to thank his government, the people of the United States and specifically the State of Montana for his educational opportunities. A traineeship from the National Aeronautics and Space Administration, the National Defense Education Act fellowship and financial assistance and equipment from the National Science Foundation were instrumental in this effort. To his advisor, Dr. J. E. Drumheller, special thanks are extended for knowledgeable instruction, wise administration and warm friendship. Thanks to Dr. David H. Dickey who constructed the machine and for the many helpful discussions. Thanks are extended to Fred Blankenburg for help with the electronics equipment and to Cecil Badgley for machine work. For the numerous acquisitions of equipment and the dependable liquid nitrogen supply, many thanks to Dr. Roy Wiegand. The writer extends appreciation to Mrs. Sheila Hight for the typescript and wonderful attention to the details in this thesis. Finally to his patient wife and children much appreciation for this wonderful opportunity.

TABLE OF CONTENTS

Table of Contents Continued

LIST OF TABLES

LIST OF FIGURES

List of Figures Continued

ABSTRACT

The temperature dependence of the intensities of the electron paramagnetic resonance (E.P.R.) spectrum for one percent Eu^{++} impurities in fluorite crystals has been investigated. This temperature dependence has been analyzed and has been shown to result from crystal expansion due to anharmonic terms of the lattice vibrations and from the harmonic terms which modulate the crystal-field as seen by the paramagnetic electrons.

It was determined that the relative intensities between forbidden and allowed hyperfine lines varied with temperature as

$$I_f/I_a = (I_f/I_a)_{T=0}(1 - CT^6 \int_0^{\Theta/T} \chi^5[\exp \chi - 1]^{-1} \, d\chi).$$

Good agreement between the predicted temperature dependence and the experiment were found; however, the value of C based on point charge calculations was subject to some question because of crystal-field parameter values.

In the analysis of the hyperfine spectrum as it depends on spatial orientation with respect to the magnetic field, certain "forbidden" hyperfine lines, heretofore not identified, were cataloged.

CHAPTER I

INTRODUCTION

The research problem in this thesis is the investigation of the temperature dependence of the intensities of the E. P. R. spectrum lines of paramagnetic europium impurities in those cubic crystals which are, for the most part, bound by coulomb forces i.e. ionic binding.

Investigations made on Eu^{++} in CaF_2 were at first concentrated on measuring the fine structure parameters and hyperfine structure parameters, (Baker, Bleaney, and Hayes, 1958 and Lacroix, 1957). The early interest also sought to give reason for the crystal-field splitting of an S-state by an electro-static field. The theories did not give numerical agreement with experiment, but did propose possible mechanisms for the splitting (Abragam and Pryce, 1951). The spin Hamiltonian of Chapter II was introduced to account for the nature of the splitting. These parameters were measured not calculated (Pryce, 1950).

Temperature dependent effects between paramagnetic ions and the crystal environment in which they may be placed were first studied theoretically. Waller (1932) in his paper "Über die Magnetisierung von Paramagnetischen Kristallen in Wechselfeldern," proposed two methods of

paramagnetic relaxation, spin-spin and the spin-lattice interactions. Fierz (1938), Kronig (1939) and Van Vleck (1939, 1940) developed this theory but found poor agreement between susceptibility experiments and the theory. The failure of the explaination by Van Vleck has been attributed to the chemistry of the alums to which he applied the theory (Manenkov and Orbach, 1966).

The advent of electron paramagnetic resonance (E.P.R.) experiments, introduced by Zaviosky (1945, 1946) and developed mainly by the Claredon Laboratory at Oxford, gave a new tool to relaxation measurements. A renewed interest in this field was a result of a paper by Finn, Orbach, and Wolf (1961). They proposed an additional process, the Orbach process, for relaxation. Van Vleck (1940) had considered the "direct" process for spin-lattice relaxation and a "Raman" process. The direct process refers to a first order effect involving a single phonon exchange between excited and ground state configurations of paramagnetic ions. The Raman process is a second order effect involving two phonons and a virtual process which allows the entire phonon spectrum to interact between two paramagnetic states. Orbach's process was simply a resonance fluorescence type process of two phonons which unlike the Raman

process includes conservation of energy.

Finn, Orbach, and Wolf's work revived an interest in spin-lattice relaxation which led to the consideration of other temperature dependent effects between phonons and the paramagnets. Blume and Orbach (1962) applied the method to S-state paramagnets and developed an orbit-lattice interaction for S-state transition metal ions. In this work they also proposed a form for the ground state splitting by a crystal field which allowed them to predict phonon contributions to the temperature dependence of crystal field splitting. The crystal field splitting in S-state transition metal ions is small while the hyperfine splitting is large. The crystal field splitting of rare-earth S-state ions is large. Eu^{++} in fluorite crystals exhibits both a large crystal field splitting and large hyperfine splitting making this ion ideal for a study of temperature dependent effects.

Temperature dependent effects of crystal field parameters have been measured by Rewaj (1968) and Horai (1964). Rewaj assumed the dependence to be due solely to lattice expansion and predicted the dependence of the parameter b_4 to be

$$b_4 = KR^{-16.3} \quad (CaF_2: \ Eu^{++}) \qquad 1.1$$

where R is the nearest neighbor ion separation. Walsh, Jeener, and Bloembergen (1965) examined the dependence of iron-group S-state ion parameters both as to temperature dependence and their dependence on R directly by subjecting the crystal to hydrostatic pressure. Because of the small value of b_4 it was not possible to tell if orbit-lattice effects contributed to the temperature dependence. Hurren, Nelson, Larson, and Gardner (1969), made similar hydrostatic pressure measurements for the crystal field parameter of CaF_2: Eu^{++} and found

$$b_4 = KR^{-8.9} \quad . \qquad 1.2$$

The difference between Rewaj's results and Hurren, et.al., suggest an orbit-lattice contribution to b_4.

In this work the dependence of b_4 on the orbit-lattice interaction was examined by measuring the temperature dependence of the intensities of the hyperfine spectrum. A similar investigation for the iron-group S-state ion was undertaken by Shrivastava and Drumheller (1969). Bir, Bulikov, and Sochara (1965) have shown the angular dependence of the hyperfine intensities depend quadratically on the crystal field parameter. In Bir's method the hyperfine transitions depend on the strong magnetic field

at the nucleus created not so greatly by the laboratory magnet but by the electronic state of the 4f shell of spin 7/2. This field, the effective field is

$$H_{eff} = \frac{A}{g_n \beta_n} \langle \Psi_e | \vec{S} | \Psi_e \rangle \quad . \qquad 1.3$$

A is the experimentally measured hyperfine coupling constant $g_n\beta_n$ is the nuclear magneton, $|\Psi_e\rangle$ are the electronic wave functions and $\vec{S}$ the spin operator for the electrons. In Chapter II the wave functions Ψ_e will be developed. Then in Chapter III the induced field method of Bir will be developed for the Eu^{++} ion in fluorite crystals. During this investigation some transitions predicted by the theory but heretofore not reported were examined. The results of this investigation are included at the end of Chapter III.

The orbit-lattice interaction was largely developed by Menne, Ames, and Lee (1968). Menne used the interaction to explain the temperature dependence of the hyperfine coupling constant A. Chapter IV will be devoted to expounding the orbit-lattice interaction and applying it to predict the temperature dependence of the hyperfine spectrum.

The results displayed in Chapter V include corrections

for crystal expansion extracted from the hydrostatic pressure measurements of Hurren. Very clear spectra were obtained in this investigation due to using the single isotope Eu^{151}. The sample obtained from A. E. C. was 96.67% Eu^{151} and 3.33% Eu^{153} with trace amounts of rare earth and other metal ions present. The crystals were grown by Optovac, Inc.

The crystal structure chosen to produce a cubic environment for the paramagnetic ion was fluorite. Examples of a fluorite crystal are CaF_2, BaF_2, and SrF_2. The unit cell of fluorite is face-centered cubic. The basis is usually an alkaline earth-halide molecule of the form ab_2. The cation a of the basis is located at (0,0,0) corner of the cube. An anion b is located at each position (1/4,1/4,1/4) and (3/4,3/4,3/4) on the diagonal of the cube.

The fluorite structure is referred to as eight-coordinated because each cation is situated in an environment of eight nearest neighbors, all anions being located at the eight corners of a cube (See Fig. 1). The crystal structure is also referred to as XY_8 to include in the reference structures of this type where the bonding may not be ionic and the X's and Y's can be a molecular

structure such as water.

Europium ions were chosen for the paramagnetic impurity because the doubly ionized atoms replace the cation of XY_8 without requiring a charge compensation elsewhere in the crystal which would change the environment of some sites from cubic to axial. The triple ionized gadolinium ion would also have an $^8S_{7/2}$ ground state such as europium but presented charge compensation problems.

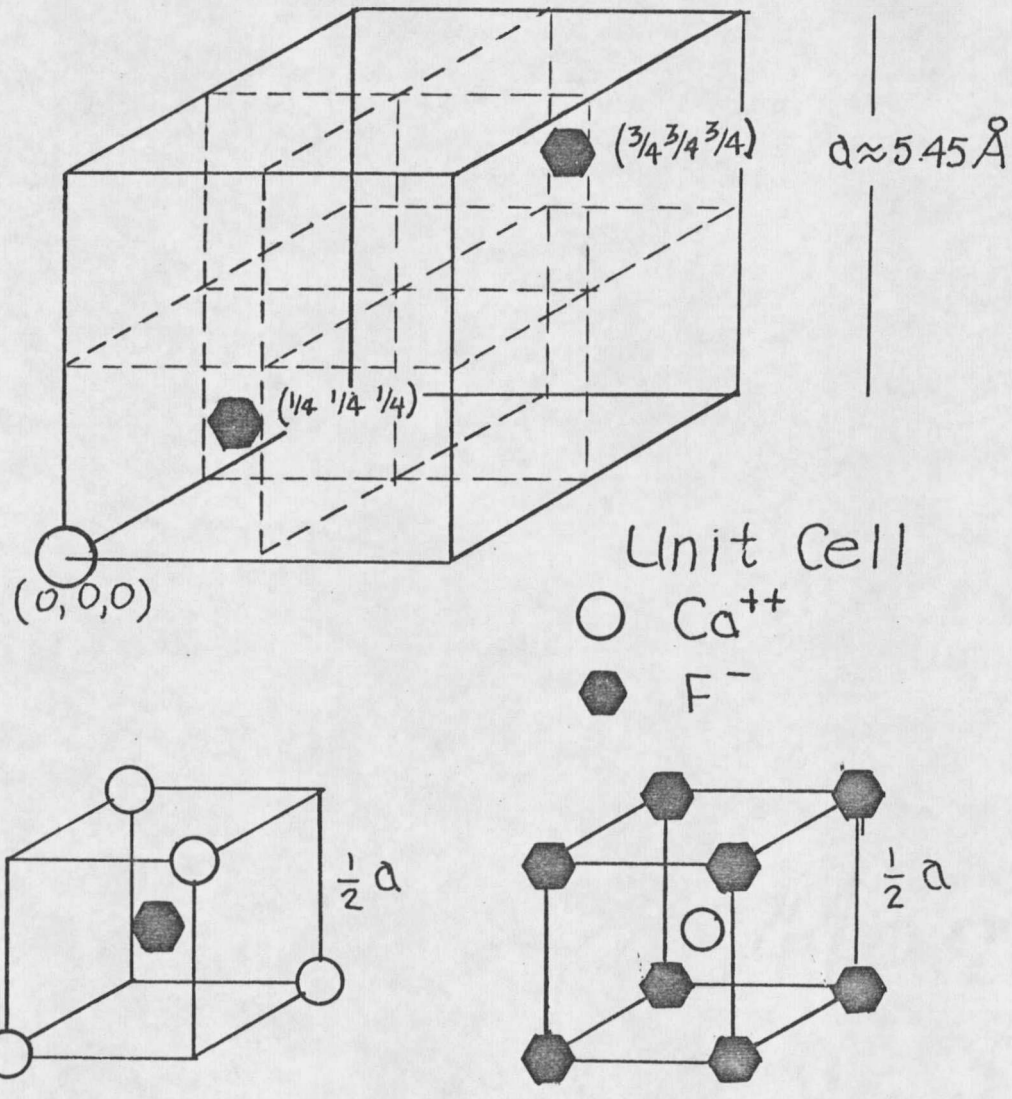

Figure 1.1

Crystallography of CaF_2 with functional cell of F and Ca ion shown.

CHAPTER II

SPLITTING OF THE $^8S_{7/2}$ GROUND STATE OF Eu IN FLUORITE CRYSTAL

Crystal Field Theory

The electric field at the paramagnetic electrons of Eu ions in a crystal is the field from all sources in the crystal. The strongest influence results from the nearest neighbor ions. A first order effect can be calculated by considering only these nearest neighbors. In order to make this calculation a very simple model is devised for the nearest neighbor interaction. First, the source ions are considered to be point sources. This assumption is much better for rare earth paramagnets than for the transition element groups because overlap of the electron wave function of the deep-seated f electron with the electronic wave function of the anion is less. The anion will henceforth be fluorine F. Second, the fluorine ions will at first be considered to be in a fixed position. This will neglect vibrations and use a time average position for the fluorine as if in a rigid lattice. Third, a semi-classical theory will be used where the electric field is calculated classically, then used as a quantum operator. Of course, any variance of this theory with an experiment

will point up the weakness of this theory and also will point to corrections which may be made to the theory (Griffith, 1961, page 65).

The Hamiltonian of the ion in a crystal including only kinetic and coulomb energies and spin-orbit effects is

$$H = \sum_{k=1}^{n} \{\frac{P_x^2}{2m} - \frac{Ze^2}{r_k} + \xi(r_k)\vec{\ell}_k \cdot \vec{S}_k + V(\vec{r}_k)\} + \sum_{k>\lambda} \frac{e^2}{r_{k\lambda}} \cdot$$

The term $V(\vec{r}_k)$ is the potential energy of the k^{th} electron in the electrostatic crystal field. The other terms are the same as for the free ion. When $V(\vec{r}_k)$ is small, the Hamiltonian can be written as

$$H = H_o + V_1$$

where V_1 is a small correction due to the Stark interaction of the electrostatic field with the ion. This form of H allows a perturbation type calculation to find the energy levels relative to the ground state free atom, and the wave function in terms of the free atom wave functions.

Using the model of Fig. 1.1 the electrostatic field at the site of a paramagnetic electron can be calculated classically considering the fluorine ions to be point sources. In this way the field point is in a charge-free region and the electric field results from a solution of

Laplace's equation

$$\nabla^2 V(r) = 0 \ . \qquad 2.1$$

The potential energy $V(\vec{r})$ of the paramagnetic electron is then

$$V(\vec{r}) = -\int \frac{e\rho(\vec{R})d\tau}{|\vec{R}-\vec{r}|} \ . \qquad 2.2$$

Choosing the paramagnetic ion as the center of the coordinate system, $\vec{R}$ is the location of the field source, i.e. the fluorine ions, and $\vec{r}$ is the location of the field point, the electrons. In rare earth atoms the assumption $\vec{R} > \vec{r}$ is valid.

$$|\vec{R}-\vec{r}| = (R^2 + r^2 - 2rR \cos \gamma)^{\frac{1}{2}}$$

Using a binomial expansion for the function $1/|\vec{R}-\vec{r}|$, $V(\vec{r})$ is

$$V(\vec{r}) = -\int \frac{e\rho(\vec{R})}{R} \sum_{\ell=0}^{\infty} \left(\frac{r}{R}\right)^{\ell} P_{\ell}(\cos \gamma)d\tau. \qquad 2.3$$

γ is the angle between $\vec{R}$ and $\vec{r}$ and the expansion coefficients are the Legendre polynomials. (Arfken, 1966, page 418).

In spherical coordinate systems the angle γ can be expressed in terms of the two different directions of $\vec{r}$

and $\vec{R}$ as

$$\cos\gamma = \cos\theta_1 \cos\theta_2 + \sin\theta_1 \sin\theta_2 \cos(\phi_1 - \phi_2),$$

ϕ's are azimuthal angles and θ's polar angles. The Legendre polynomial P_ℓ can be expanded in terms of spherical harmonics by the addition theorem (Arfken, 1966, page 450-453)

$$P_\ell(\cos\gamma) = \frac{4\pi}{2\ell+1} \sum_{m=-\ell}^{\ell} (-1)^m Y_\ell^m(\theta_1,\phi_1) Y_\ell^{-m}(\theta_2,\phi_2). \qquad 2.4$$

(Also see Messiah I, 1961 Appendix B).

$$V(\vec{r}) = 4\pi \int \frac{e\rho(R)d\tau_2}{R} \sum_{\ell=0}^{\ell} \left(\frac{r}{R}\right)^\ell \frac{1}{2\ell+1} \times$$

$$\sum_{m=-\ell}^{\ell} (-1)^m Y_\ell^m(\theta_1,\phi_1) Y_\ell^{-m}(\theta_2,\phi_2). \qquad 2.5$$

Group Theory

The point group symmetry of XY_8 is O_h. O_h refers to the point group operations performed on a cube which cannot be distinguished from the unaffected cube. The set of elements of this group contains an identity, the unchanged cube; a 180° rotation about an axis perpendicular to each face of the cube and passing through the center of the cube; a 180° rotation about each axis passing through the midpoint of an edge and the center of the cube;

two 120° rotations, clockwise and counter-clockwise, about each of the cube diagonals; and two 90° rotations about each face axis, clockwise and counter-clockwise. Also included in O_h are the improper rotations or each of the proper rotations mentioned above followed by an inversion.

The elements of the O_h point group can be grouped as classes, these being the identity class, the 120° rotation class of which there are eight elements, the two 180° rotation classes, the face centered class of three elements, and the edge centered class of six elements; the six 90° elements form a class as do the improper rotations associated with each class above. If the elements are represented by rotation matrices, the elements of the same class all have the same trace. The trace is called the character of the class and the point group.

There is only a finite number of ways in which a finite abstract group can be made to represent the group in terms of concrete mathematical entities. Any one way is called a "representation" of the group and the number of irreducible representations equals the number of classes. A representation is said to be irreducible if it cannot be expressed as the outer product of representation

of lesser dimensionality. A character table for O_h is given in Appendix A. An irreducible representation in terms of the characters of the classes is given for the possible matrix representations of the group.

The abstract group of rotations has been represented by rotation matrices. These matrices transform functions within a finite dimensional subspace among themselves and if no set of functions within this manifold, apart from the whole subspace, were to transform among themselves by the group operations, the subspace would be irreducible (Gel'fand, Minlos, and Shapiro, 1963, page 16. Also see Appendix A). The basis functions which are transformed by the group elements, form a Euclidean space. Writing these functions analytically can be accomplished an infinite number of ways. The functions can be, however, an orthogonal set. The functions are a "basis" of the representation chosen and must transform distinctly among themselves by the operations of the group. Given any function as one of the basis functions all the basis for the other representations can be generated orthogonal to one another (Tinkham, 1964, page 41).

The set of all rotations is an infinite group and the set of spherical harmonics form a set of basis functions

for the full rotation group. The spherical harmonics of the same order ℓ are

$$Y_\ell^m(\theta,\phi) = (-1)^m \left[\frac{(2\ell+1)(\ell-m)!}{4\pi \quad (\ell+m)!}\right] P_\ell^m(\cos\theta) e^{im\phi}$$

where θ is the polar angle and ϕ the azimuthal angle in spherical coordinates. P_ℓ^m are associated Legendre polynomials, and $-\ell \leq m \leq \ell$ (Messiah, 1961, page 495). A transformation by a spatial rotation transforms the Y_ℓ^m's of order ℓ among themselves.

$$Y_\ell^{m'} = \sum_{n=-\ell}^{\ell} C_{mn}^{\ell} Y_\ell^n \quad , \qquad 2.6$$

then the C_{mn}^{ℓ}'s are matrix elements as calculated in Appendix A. By the definition of an irreducible representation, any set of $2\ell+1$ spherical harmonic of order ℓ form a basis for the full rotation group since they transform among themselves.

The crystalline field transforms according to its own identity representation (Γ_{1g}) for O_h. Only $D^{(0)}$, $D^{(4)}$, $D^{(6)}$, $D^{(8)}$... contain Γ_{1g} when reduced under O_h. Thus in the crystal field expansion in terms of spherical harmonics (Eq. 2.5) only the ℓ = 0, 4, 6, 8, ... need be kept. The 4f electrons of Eu^{+2} will have spherical functions of ℓ = 3. Non-zero matrix elements will result from direct products

$D^{(3)} \times D^{(\ell)} \times D^{(3)}$; $D^{(\ell)}$ being the matrix of the crystal field. It can be seen that

$$D^{(3)} \times D^{(\ell)} \times D^{(3)} = D^{(\ell)} \times$$

$$[D^{(6)} + D^{(5)} + D^{(4)} + D^{(3)} + D^{(2)} + D^{(1)} + D^{(0)}]$$

thus no non-zero matrix will result for $\ell > 6$, since only $D^{(6)} \times D^{(6)}$ contain $D^{(0)}$.

The $\ell = 0$ spherical functions are not angular dependent and only add a constant to the potential energy term $V(\vec{r})$. Then

$$V(\vec{r})_{cubic} = \sum_{\ell=0}^{\infty} \sum_{m=-\ell}^{\ell} r^{\ell} \gamma^{\ell m} Y_{\ell}^{m} \qquad 2.7$$

where from eq. 2.2 and 2.5

$$\gamma^{\ell m} = - \frac{4\pi e}{(2\ell+1)R^{\ell+1}} \int Y_{\ell}^{-m} (\theta_2 \phi_2) d\tau_2 \rho(R).$$

Eq. 2.7 becomes

$$V(\vec{r})_{cubic} = r^4 \left[\sum_{m=-4}^{4} \gamma^{4m} Y_4^m \right] + r^6 \left[\sum_{m=-6}^{6} \gamma^{6m} Y_6^m \right].$$

The rotation about the z axis of $\pi/2$ transforms the coordinate system as:

$$x \to y, \; y \to -x, \text{ and } z \to z.$$

The spherical functions Y_4^0, Y_4^4, and Y_4^{-4} are the only

invariants of order 4 under this transformation. Y_6^0 and $Y^{\pm 4}_6$ are the only order 6 invariants (Low, 1960, Table II).

Considering point charges and XY_8

$$V(\vec{r}) = \frac{-Ze^2r^4}{R^5}\ \frac{4\pi}{9}\left[\frac{28}{9}Y_4^0 + \frac{2}{9}\sqrt{70}\,(Y_4^4 + Y^{-4}_4)\right]$$

$$+ \frac{Ze^2r^6}{R^7}\ \frac{4\pi}{13}\left[\frac{16}{9}Y_6^0 + \frac{8}{9}\sqrt{14}\,(Y_6^4 + Y^{-4}_6)\right]$$

which may be written as

$$V(\vec{r}) = B_4(0_4^0 + 50_4^4) + B_6(0_6^0 - 210_6^4) \qquad 2.8$$

0_ℓ^m is the sum $Y_\ell^m + Y^{-m}_\ell$ in which any common numerical factors have been taken out and included in B (Jones, Baker and Pope, 1959 and Stevens, 1952).

Operator Equivalence

A vector $\vec{T}$ can be defined as a vector of type "T" following Condon and Shortley (1935), with respect to a general angular momentum $\vec{j}$ when it meets the following commutation relations:

$$\left[j_\ell, T_m\right] = ihT_n\varepsilon_{\ell mn}.$$

$\varepsilon_{\ell mn}$ is the Levi-Civita tensor density (Goldstein, 1959, page 129), defined to be zero if any two of the indices ℓ, m, n are equal, and either +1 or -1 otherwise, according

as (ℓ, m, n) is an even or odd permutation of (x, y, z). Two excellent expositions of the subject of angular momentum in quantum mechanics can be found in Chapter II of J. S. Griffith's The Theory of Transition-Metal Ions (1961) and Chapter XII of A. Messiah's Quantum Mechanics, Volume II (1962).

The replacement theorem follows from the Wigner-Eckart theorem and says that if $\vec{T}_1$ and $\vec{T}_2$ are both type T with respect to $\vec{j}$ then $\langle\alpha' jm|\vec{T}_1|\alpha'' j'm'\rangle = \gamma\langle\alpha' jm|\vec{T}_2|\alpha'' jm'\rangle$ where $\gamma = \gamma(\alpha'\alpha, j'j)$ independent of m and m'. A corollary to the replacement theorem is:

For any vector $\vec{T}$ of type T with respect to $\vec{j}$, the relation

$$\langle\alpha' jm|\vec{T}|\alpha'' jm'\rangle = \gamma\langle\alpha' jm|\vec{j}|\alpha' jm'\rangle \qquad 2.9$$

holds with $\gamma = \gamma(\alpha', \alpha'', j)$. Note on the right side of the equation the quantum numbers j and α' are the same for both bra and ket. This results because any component of $\vec{j}$ can only generate functions within the manifold of 2j+1 eigenstates belonging to j and α'. The manner of using this theorem and the corollary would be to evaluate γ for any one matrix element then use the replacement theorem.

The replacement theorem allows the crystal field operator in terms of the spherical functions Y_ℓ^m to be

replaced by angular momentum operators. If the spherical functions are written in terms of their cartesian equivalents, each of the components x, y, and z can be replaced by operator equivalents in j_x, j_y, and j_z. These operators are to be expressed in a standard representation whose basis vectors are the set $|\alpha jm\rangle$, that is in the normalized

$$j_1 = \frac{1}{\sqrt{2}} (j_x + ij_y) = \frac{1}{\sqrt{2}} j_+$$

$$j_0 = j_z$$

$$j_{-1} = \frac{1}{\sqrt{2}} (j_x - ij_y) = \frac{1}{\sqrt{2}} j_- \qquad 2.10$$

Because of the noncommuting nature of the operators, mixed products such as xy must be symmetrized when replaced by operator equivalents, for example:

$$xy \rightarrow 1/2\ (xy + yx) \rightarrow 1/2\gamma\ (j_x j_y + j_y j_x).$$

The crystal field written in operator equivalent form is from eq. 2.8,

$$V(\vec{r}) = B_4(O_4^0 + 5O_4^4) + B_6(O_6^6 - 21O_6^4) \qquad 2.11a$$

$$O_4^0 = 35j_z^4 - 30j(j+1)j_z^3 + 25j_z^2 - 6j(j+1) + 2j^2(j+1)^2,$$

$$O_4^4 = \frac{1}{2}\left[j_+^4 + j_-^4\right] \qquad 2.11b$$

$$O_6^0 = 231\, j_z^6 - 315j(j+1)\, j_3^4 + 105j^2(j+1)^2 j_3^2 - 525j(j+1)j_z^2 + 294j_z^2 - 5j^3(j+1)^3 + 40j^2(j+1)^2 - 60j(j+1) \qquad 2.11c$$

$$O_6^4 = \frac{1}{4}\left[(j_+^4 + j_-^4)\{11j_z^2 - j(j+1) - 38\} + \{11j_z^2 - j(j+1) - 38\}(j_+^4 + j_-^4)\right] . \qquad 2.11d$$

(Jones, Baker, and Pope, 1959, Table 3).

The Spin Hamiltonian

The angular momentum of the europium ion is $\vec{J} = \vec{L}+\vec{S}=\vec{S}$. The shells are all closed with respect to orbital angular momentum. In the above notation then, replace $\vec{j}$ with $\vec{S}$. A difficulty results since $\vec{S}$ is not a T type vector with respect to $\vec{L}$. The result of this is to nullify the replacement theorem. Physically, this result states that the Stark effect cannot split a system which has a closed electron shell.

Group theory, which explains the type of splitting allowed if the mechanism were present, predicts a crystal field splitting of three levels. The O_h group must now be a double group to account for the nature of half integral angular momentum systems where a twofold rotation

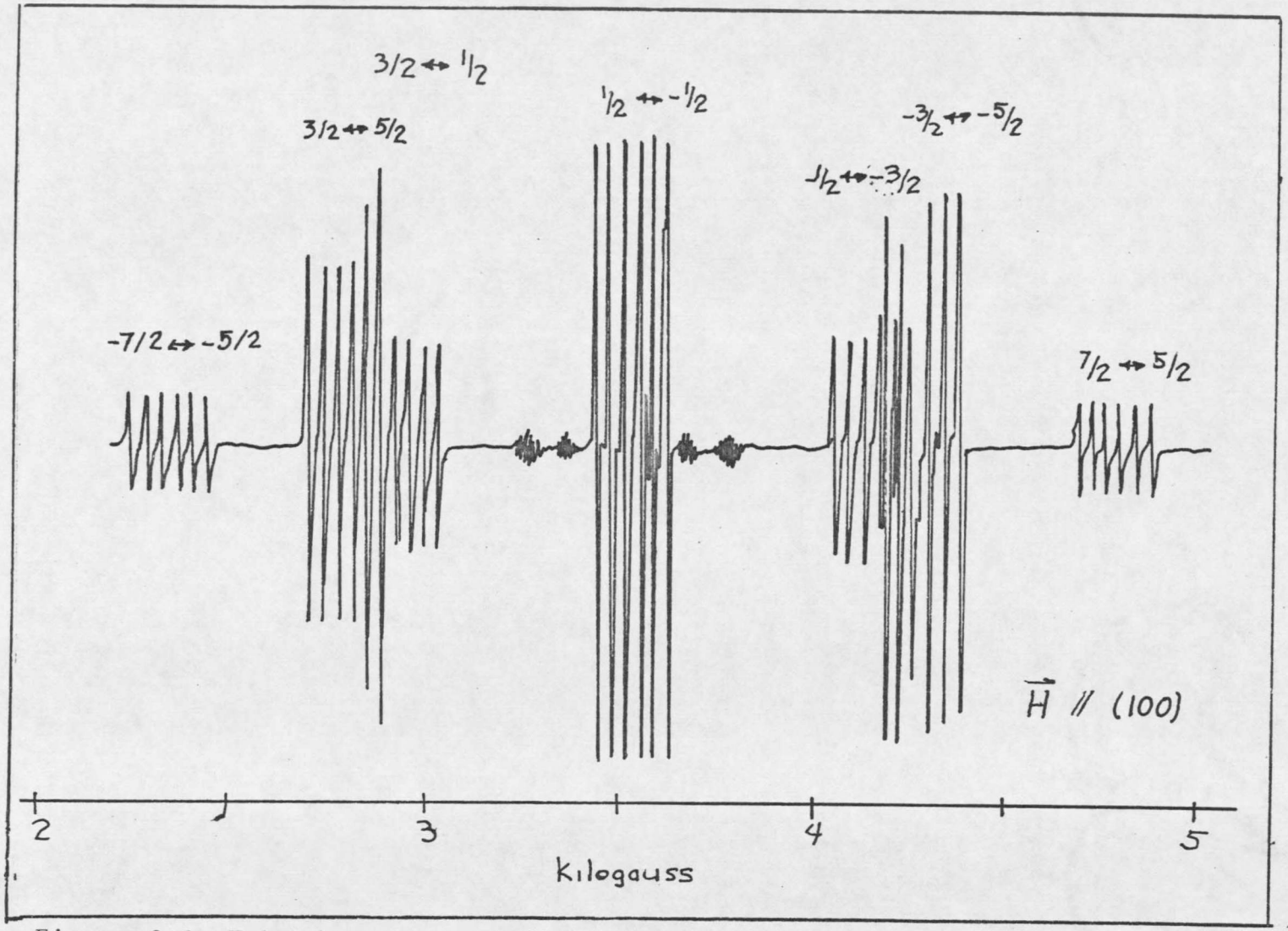

Figure 2.1 X-band spectrum 0.1% Eu - CaF_2 at 78°K.

is single valued. The zero magnetic field splitting of a J = 7/2 system is calculated in Appendix A.

Experimental evidence clearly shows there is a crystal field interaction. Fig. 2.1 shows the splitting of the ground state by a Zeeman effect. The fine structure spectrum can only be explained if a crystal field interaction exists. This splitting will be calculated below and the energy level diagram of Fig. 2.2 shows the zero field splitting.

An explanation of the S-state splitting by Van Vleck and Penney (1934) concluded that an orbit-spin coupling mixed in excited states in which L is not zero. Abragam and Pryce (1951) considered the spin-spin interaction between dipoles which depends on spin variables and position variables

$$H_{spin\text{-}spin} = \left| \vec{S}_j \cdot S_k / r_{ik}^3 - \frac{3(\vec{r}_{jk} \cdot \vec{S}_j)(\vec{r}_{jk} \cdot \vec{S}_k}{r_{jk}^5} \right| . \qquad 2.12$$

The crystal field distorts the orbits which are coupled to other spins resulting in a net distortion of the ground state. The distorted S-state can interact whith the electric field.

An acceptable theory which shows good agreement with

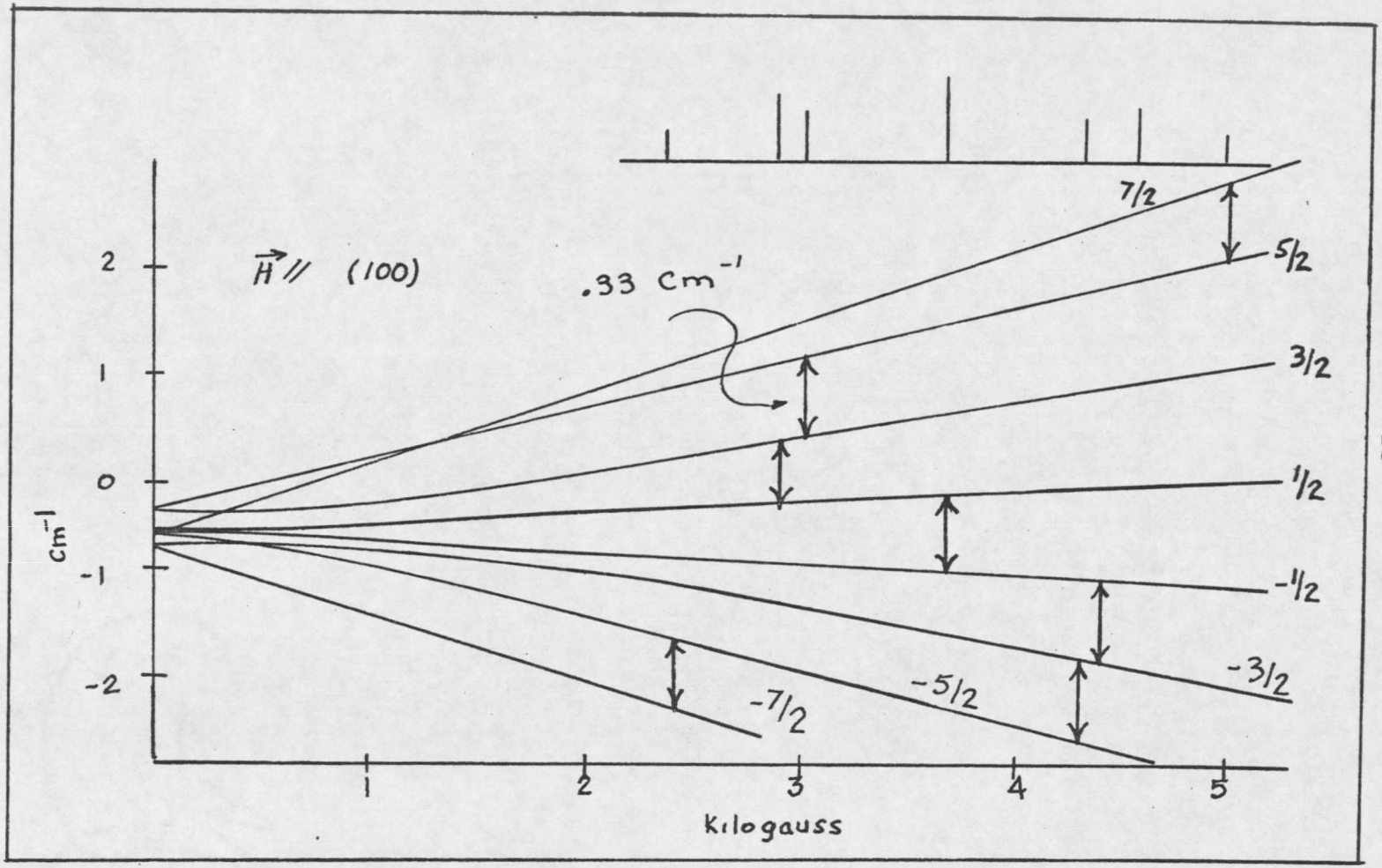

Figure 2.2 Fine structure splitting Eu - CaF_2 as a function of magnetic Field.

the experiments on S-states has not been developed to date. An heuristic Hamiltonian can be proposed in which the coefficients B_4 and B_6 of eq. 2.8 are measured experimentally. This is the "Spin Hamiltonian" for S-state ions.

$$H = g\beta\vec{H}\cdot\vec{S} + B_4(0_4^0 + 50_4^4) + B_6(0_6^0 - 210_6^4) + \vec{I}\cdot\vec{A}\cdot\vec{S} + g_n\beta_n\vec{H}\cdot\vec{I}. \qquad 2.13$$

$g\beta\vec{H}\cdot\vec{S}$ is the Zeeman effect of a magnetic dipole $g\beta\vec{S} = \vec{\mu}_e$ in a magnetic field. There is also a nuclear Zeeman term $g_N\beta_N\vec{H}\cdot\vec{I}$ which is small compared to other spin Hamiltonian terms but is kept in order to devise nuclear wave functions required to explain the hyperfine interaction (see Chapter III).

An interaction between the electrons and the nucleus is called the hyperfine interaction. This interaction is essentially a spin-spin interaction as eq. 2.12. An s electron has a finite probability of being within the nuclear volume giving rise to the Fermi contact term

$$(8\pi/3)\, g\beta g_N\beta_N\, \delta(\vec{r}_e - \vec{r}_n)\, \vec{I}\cdot\vec{S}\ .$$

F. J. Milford (1960) has a simple derivation of this term in the American Journal of Physics.

The spin-spin term of the hyperfine interaction does not predict as large a hyperfine coupling tensor $\vec{A}$, which

is a constant for Eu, as is measured in experiments. William Hayes (1963) accounts for the hyperfine interaction as resulting mostly from the Fermi contact term of unpaired s electrons density at the nucleus. In Eu all the s electrons are paired, thus no hyperfine splitting should occur. It is thought, however, that the unfilled paramagnetic shell will polarize the s electrons by exchange interactions such that one of the pair will have a greater electron density in the nucleus than the other. The hyperfine interaction is included as a spin Hamiltonian term and A is measured by experiment (Baker, Bleaney, and Hayes, 1958).

Fine Structure

Taking the Hamiltonian

$$H = g\vec{H}\cdot\vec{S} + B_4(O_4^0 + 5O_4^4) + B_6(O_6^0 - 21O_6^4),$$

the crystal field dominates when $\vec{H}$ is small and group theory predicts a zero field splitting. Replacing the operators O by spin operators in a standard representation as given in Table II, and evaluating matrix elements between the basis of the representation, $|SM_s>$, an eight by eight martix results. The matrix has four distinct diagonal elements. $<S,M|H_{cf}|S,M> = <S,-M|H_{cf}|S,-M>$, a

result which stems from Kramer's theorem (Tinkham, 1964, page 143.) For any half-integral angular momentum system an electric field of any symmetry can at best remove degeneracy such that each new level is of even degeneracy. This is because an electric field results from a time reversal symmetry. The matrix can be written as two four by four matrices along the diagonal. The cubic field operators 0 only have off-diagonal elements between M and M ±4 by virtue of the terms S_+^4 and S_-^4. By an interchange of rows and columns the 4 x 4 matrix becomes two 2 x 2 matrices along the diagonal.

Figure 2.3

	±7/2	±1/2		
±7/2	$(7b_4+b_6)$	$35(b_4-3b_6)$	0	0
±1/2	$35(b_4-3b_6)$	$(9b_4-5b_6)$	0	0
±5/2	0	0	$(-13b_4-5b_6)$	$3(5b_4+7b_6)$
±3/2	0	0	$3(5b_4+7b_6)$	$(-3b_4+9b_6)$

where $b_4 = 60B_4$ and $b_6 = 120B_6$ of eq. 2.13.

By diagonalizing the above matrix the eigenvalues of energy are

$$E_1 = 14b_4 - 20b_6, \quad M = \pm 5/2,$$

$$E_2 = 2b_4 + 16b_6, \quad M = \pm 7/2,$$

$$E_3 = 2b_4 + 16b_6, \quad M = \pm 3/2,$$

and $$E_4 = -18b_4 - 12b_6, \quad M = \pm 1/2.$$

The E_2 and E_3 levels are degenerate, and since each level is twofold degenerate because of Kramer's degeneracy, two twofold degenerate levels and a four fold level are split by a zero magnetic field Hamiltonian.

Figure 2.4

Zero Field Splitting

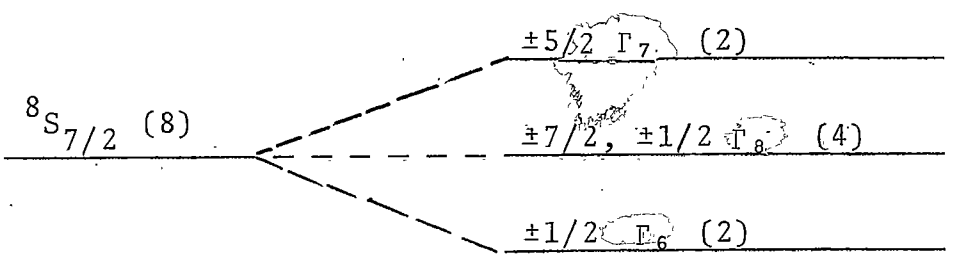

If a magnetic field is introduced such that the field is directed along the z axis of the crystal field (±x, ±y, ±z are equivalent z axes) the spin Hamiltonian is

$$H = g \vec{H} \cdot \vec{S} + \frac{b_4}{60} (0_4^0 + 50_4^4) + \frac{b_6}{1260} (0_6^0 - 210_6^4)$$

when the magnetic field is small the states are perturbed

by $H_1 = g\beta H S_z$ which removes the remaining degeneracy.

In the strong field region, the crystal field term is the perturbation and the eigenfunctions belonging to S_z are perturbed by

$$V_{cf} = \frac{b_4}{60}\,(O_4^0 + 5O_4^4) + \frac{b_6}{1260}\,(O_6^0 - 21O_6^4). \qquad 2.14$$

Figure 2.2 displays the splitting as a function of the field strength H.

The eigenvalues of H when considering eq. 2.14 as a small H_1, $H_1 \ll g\beta H$ are

$$E_M = E_M^0 + \langle M|H_1|M\rangle + \sum_{M'}{}' \frac{\langle M|H_1|M'\rangle\langle M'|H_1|M\rangle}{E_M^0 - E_{M'}^0} \qquad 2.15$$

with

$$E_M^0 = \langle M|g\beta H S_z|M\rangle = g\beta H M.$$

The eigenfunctions belonging to S_z are $|\alpha SM\rangle$. These are shortened to $|M\rangle$ within the manifold $S = 7/2$ for Eu ions; $-7/2 \leq M \leq 7/2$. The resulting levels are

$$E_{\pm 7/2} = \pm g\beta H(7/2) + 7b_4 + b_6 \pm \frac{35(b_4 - 3b_6)^2}{4g\beta H} \qquad 2.16a$$

$$E_{\pm 5/2} = \pm g\beta H(5/2) - 13b_4 - 5b_6 \pm \frac{3(5b_4 + 7b_6)^2}{4g\beta H} \qquad 2.16b$$

$$E_{\pm 3/2} = \pm g\beta H(3/2) - 3b_4 + 9b_6 \pm \frac{3(5b_4+7b_6)^2}{4g\beta H} \qquad 2.16c$$

and

$$E_{\pm 1/2} = \pm g\beta H(1/2) + 9b_4 - 5b_6 \pm \frac{35(b_4-3b_6)^2}{4g\beta H} \qquad 2.16d$$

Angular Dependence of Fine Structure.

When the coordinates x, y, and z of the crystalline field do not coincide with the vector external magnetic field, the vector products of eq. 2.13 must be written in a common coordinate system. In eq. 2.13 it is implied that the coordinate system chosen is along the three equivalent crystal axes. Maintaining this coordinate system, the scalar product $\vec{H}\cdot\vec{S}$ becomes

$$\vec{H}\cdot\vec{S} = H(S_x \sin\theta \cos\phi + S_y \sin\theta \sin\phi + \cos\theta).$$

In the experiment the magnetic field $\vec{H}$ was always at right angles to a (100) axis of the crystal. In the calculations the rotations are always in the x, z plane; thus the azimuthal angle ϕ is zero. The terms of the matrix of figure 2.5 times $g\beta H$ are the matrix elements of H of eq. 2.13. b_4' and b_6' are respectively $b_4/g\beta H$ and

	-7/2	-5/2	-3/2	-1/2	1/2	3/2	5/2	7/2
$-\frac{7}{2}$	$7b_4+b_6$ $-7/2\cos\theta$	$\sqrt{7}/2\sin\theta$	0	0	$\sqrt{35}$ (b_4-3b_6)	0	0	0
$-\frac{5}{2}$	$\sqrt{7}/2\sin\theta$	$-13b_4-5b_6$ $-5/2\cos\theta$	$\sqrt{3}\sin\theta$	0	0	$\sqrt{75}$ $(b_4+7/5b_6)$	0	0
$-\frac{3}{2}$	0	$\sqrt{3}\sin\theta$	$-3b_4+9b_6$ $-3/2\cos\theta$	$\frac{\sqrt{15}}{2}\sin\theta$	0	0	$\sqrt{75}$ $(b_4+7/2b_6)$	0
$-\frac{1}{2}$	0	0	$\sqrt{15}/2$ $\sin\theta$	$9b_4-5b_6$ $-1/2\cos\theta$	$2\sin\theta$	0	0	$\sqrt{35}$ (b_4-3b_6)
$\frac{1}{2}$	$\sqrt{35}$ (b_4-3b_6)	0	0	$2\sin\theta$	$9b_4-5b_6$ $1/2\cos\theta$	$\frac{\sqrt{15}}{2}\sin\theta$	0	0
$\frac{3}{2}$	0	$\sqrt{75}$ $(b_4+7/5b_6)$	0	0	$\frac{75}{2}\sin\theta$	$-3b_4+9b_6$ $+3/2\cos\theta$	$\sqrt{3}\sin\theta$	0
$\frac{5}{2}$	0	0	$\sqrt{75}$ $(b_4+7/5b_6)$	0	0	$\sqrt{3}\sin\theta$	$-13b_4-5b_6$ $5/2\cos\theta$	$\frac{\sqrt{7}}{2}\sin\theta$
$\frac{7}{2}$	0	0	0	$\sqrt{35}$ (b_4-3b_6)	0	0	$\frac{\sqrt{7}}{2}\sin\theta$	$7b_4+b_6$ $+7/2\cos\theta$

Figure 2.5

$b_6/g\beta H_o$, the angle θ is the angle between a (100) axis of the crystal, chosen as the z axis of the coordinate system, and the magnetic field $\vec{H}_o$. The resulting matrix is displayed in Fig. 2.5.

An approximate diagonalization of this matrix using perturbation techniques can be used when $H_o \ll 60$ gauss. Using a much larger field, H_o, it is possible to treat the crystal field as a perturbation as in eq. 2.16; however, a representation written with the z axis along the H_o direction is then necessary. In this case the crystal field operators 0 written in the cartesian form for the spherical harmonics will transform as

$$x \rightarrow x \sin\theta \rightarrow S_x \sin\theta \rightarrow \frac{S_+ + S_-}{2} \sin\theta$$

and

$$z \rightarrow z \cos\theta \rightarrow S_z \cos\theta$$

where again all products of S_z, S_+, and S_- must be symmetrized. This has been done for the operators 0_4^0, 0_4^4, 0_6^0, 0_6^4 of eq. 13, (Stevens, 1951 and Jones, Baker, and Pope).

Table 2.1

Jones, Baker, and Pope (1959)

$$O_4^0 \rightarrow \frac{3}{8} O_4^0 + \frac{5}{2} O_4^2 + \frac{35}{8} O_4^4$$

$$O_4^2 \rightarrow \left(-\frac{1}{8} O_4^0 - \frac{1}{2} O_4^2 + \frac{7}{8} O_4^4\right) \cos 2\phi + i\left(\frac{1}{2} O_4^1 + \frac{7}{2} O_4^3\right) \sin 2\phi$$

$$O_4^4 \rightarrow \left(\frac{1}{8} O_4^0 - \frac{1}{2} O_4^2 + \frac{1}{8} O_4^4\right) \cos 4\phi - i(O_4^1 - iO_4^3) \sin 4\phi$$

$$O_4^4 \rightarrow -\frac{5}{16} O_6^0 - \frac{105}{32} O_6^2 - \frac{63}{16} O_6^4 - \frac{231}{32} O_6^6$$

$$O_6^2 \rightarrow \left(\frac{1}{16} O_6^0 + \frac{17}{32} O_6^2 + \frac{3}{16} O_6^4 - \frac{33}{32} O_6^6\right) \cos 2\phi$$
$$-i\left(\frac{1}{4} O_6^1 + \frac{9}{8} O_6^3 + \frac{33}{8} O_6^5\right) \sin 2\phi$$

$$O_6^4 \rightarrow \left(-\frac{1}{16} O_6^0 - \frac{5}{32} O_6^2 + \frac{13}{16} O_6^4 - \frac{11}{32} O_6^6\right) \cos 4\phi$$
$$+i\left(\frac{1}{2} O_6^1 + \frac{5}{4} O_6^3 - \frac{11}{4} O_6^5\right) \sin 4\phi$$

$$O_6^6 \rightarrow \left(\frac{1}{16} O_6^0 - \frac{15}{32} O_6^2 + \frac{3}{16} O_6^4 - \frac{1}{32} O_6^6\right) \cos 6\phi$$
$$-i\left(\frac{3}{4} O_6^1 - \frac{5}{8} O_6^3 + \frac{3}{8} O_6^5\right) \sin 6\phi$$

The Hamiltonian with an angle θ between the crystal axis and the magnetic field (chosen to be the z axis of coordinate system) rotated about the y axis is

$$H = g\beta HS_z + \frac{b_4}{60}\{\frac{3}{8}O_4^0 + \frac{5}{8}O_4^2 + \frac{35}{8}O_4^4 + 5[(\frac{1}{8}O_4^0 - \frac{1}{2}O_4^2 + \frac{1}{8}O_4^4)\cos 4\theta - i(O_4^1 - iO_4^3)\sin 4\theta]\} + \frac{b_6}{1260} \times\{-\frac{5}{16}O_6^0 - \frac{105}{32}O_6^2 - \frac{63}{16}O_6^4 - \frac{231}{32}O_6^6 - 21[(-\frac{1}{16}O_6^0 + \frac{13}{16}O_6^4 - \frac{11}{16}O_6^6)\cos 4\theta + i(\frac{1}{2}O_6^1 + \frac{5}{4}O_6^3 - \frac{11}{4}O_6^5)\sin 4\theta]\} \qquad 2.17$$

Tables giving the values of the matrix elements of the O_m^n 's are given by Low (1960) and Drumheller (1969).

A concluding note to give further insight into the transformation of the O_m^n 's follows. The O_m^n's are a linear combination of O_m^{n+} and O_m^{n-} which are spherical harmonics written in symmetrized operator equivalent form. The common numerical coefficients are not included. On rotation the spherical harmonics Y_ℓ^m are transformed into linear combinations of the spherical harmonics belonging to the same manifold ℓ:

$$Y_\ell^m(\theta',\phi') = \sum_n C_{mn}^\ell \, Y_\ell^n(\theta,\phi). \qquad 2.6$$

The transformation matrix whose elements are the C_{mn}^ℓ 's is unitary. This matrix is the operator

$$e^{-i\phi(\vec{J}\cdot\vec{\mu})} |\ell m\rangle = R(\phi) \, |\ell m\rangle \qquad 2.18$$

Table 2.2

Jones, Baker, and Pope (1959)
Baker, Bleaney, and Hayes (1951)

Form of Operators O_n^m

$$O_4^0 = 35S_z^4 - [30S(S+1) - 25]S_z^2 - 6S(S+1) + 3S^2(S+1)^2$$

$$O_4^2 = \tfrac{1}{4}[\{7S_z^2 - S(S+1) - 5\}(S_+^2+S_-^2) + (S_+^2+S_-^2)\{7S_z^2-S(S+1)-5\}]$$

$$O_4^4 = \tfrac{1}{2}(S_+^4 + S_-^4)$$

$$O_6^0 = 231S_z^6 - 105\{3S(S+1)-7\}S_z^4 + \{105S^2(S+1)^2-525S(S+1) + 294\}S_z^2$$
$$-5S^3(S+1)^3 = 40S^2(S+1)^2 - 60S(S+1)$$

$$O_6^2 = \tfrac{1}{4}[\{33S_z^4-[18S(S+1)+123]S_z^2(S+1)^2+10S(S+1)+102\}(S_+^2 + S_-^2)$$
$$+ (S_+^2 + S_-^2)\{33S_2^4 - \text{etc.}\}]$$

$$O_6^4 = \tfrac{1}{4}[\{11S_z^2 - S(S+1)-38\}(S_+^4 + S_-^4) + (S_+^4 + S_-^4)\{11S_z^2-S(S+1)-38\}]$$

$$O_6^6 = \tfrac{1}{2}(S_+^6 + S_-^6)$$

$$O_4^3 = (\tfrac{1}{4})\{S_z(S_+^3 + S_-^3) + (S_+^3 + S_-^3)S_z\}$$

$$O_6^3 = \tfrac{1}{4}\{[11S_z^3-3S(S+1)S_z-59S_z](S_+^3 + S_-^3)+(S_+^3+S_-^3)[11S_z^3-$$
$$-3S(S+1)S_z-59S_z]\}$$

$$O_6^2 = \tfrac{1}{4}\{[35S_z^5-S_z^3\langle 30S(S+1)-15\rangle+S_z\langle 5S^2(S+1)^2-105(S+1)+12\rangle](S_+ + S_-)$$
$$+ (S_+ + S_-)[35S_z^5-S_z^3\langle 30S(S+1)-15\rangle+S_z\langle 5S^2(S+1)-105(S+1)+12\rangle]\}$$

$$O_4^1 = \tfrac{1}{4}\{[7S_z^3-35(S+1)S_z-S_z](S_+ + S_-)+(S_+ + S_-)[7S_z^3(S+1)S_z-S_z]\}$$

ϕ is the angle of rotation, $\vec{J}$, the angular momentum operator and $\vec{\mu}$ a unit vector acting as the axis of rotation. (Messiah, 1964 Appendix D, Section 10 and Chapter XIII). Gel'fand, Minlos, and Shapiro (1963) derive this operator in terms of Euler angles. The solution is the Generalized Spherical Functions which are also used in Chapter III to explain the hyperfine interaction. The function is derived in Appendix A.

Baker, Bleaney, and Hayes (1958) have used first order perturbation calculations to find the angular dependence of the fine structure energy levels. In eq. 2.16 the following substitutions are made to show this dependence (Bleaney, Baker, and Hayes, 1958):

$$b_4 \rightarrow b_4\, p; \quad b_6 \rightarrow b_6\, q, \tag{2.19}$$

where

$$p = 1 - 5(\ell^2 m^2 + m^2 n^2 + n^2 \ell^2)$$

and

$$q = \frac{21}{2}\{11\ell^2 m^2 n^2 - (\ell^2 m^2 + m^2 n^2 + n^2 \ell^2) + \frac{2}{21}\}. \tag{2.20}$$

In eq. 2.20 (ℓ, m, n) are the direction cosines to the (x,y,z) axis. In spherical coordinates

$$\ell = \sin\theta \cos\theta$$
$$m = \sin\phi \sin\phi$$

and

$$n = \cos \theta,$$

Since the rotations of the experiment are made in the x-z plane, the azimuthal angle ϕ is $\pi/2$ thus

$$p = 1 - \frac{5}{4} \sin^2 \theta \cos^2 \theta = 1 - \frac{5}{16} \sin^2 2\theta$$

$$q = 1 - \frac{21}{8} \sin^2 2\theta.$$

The angular dependence of the difference between adjacent levels (since transitions between these levels were the measured quantities in the experiment, the differences $\Delta M \pm 1$ are plotted rather than the energy levels themselves) is plotted in Fig. 2.6.

When Θ is zero the fine structure transitions of eq. 16 are plotted in Fig. 2.2 when the energy difference between $\Delta M \pm 1$ levels is 0.33 cm^{-1} in energy (the 10 GHz microwave energy). This figure shows the location of the high field splitting of the fine structure levels which result from eq. 2.16.

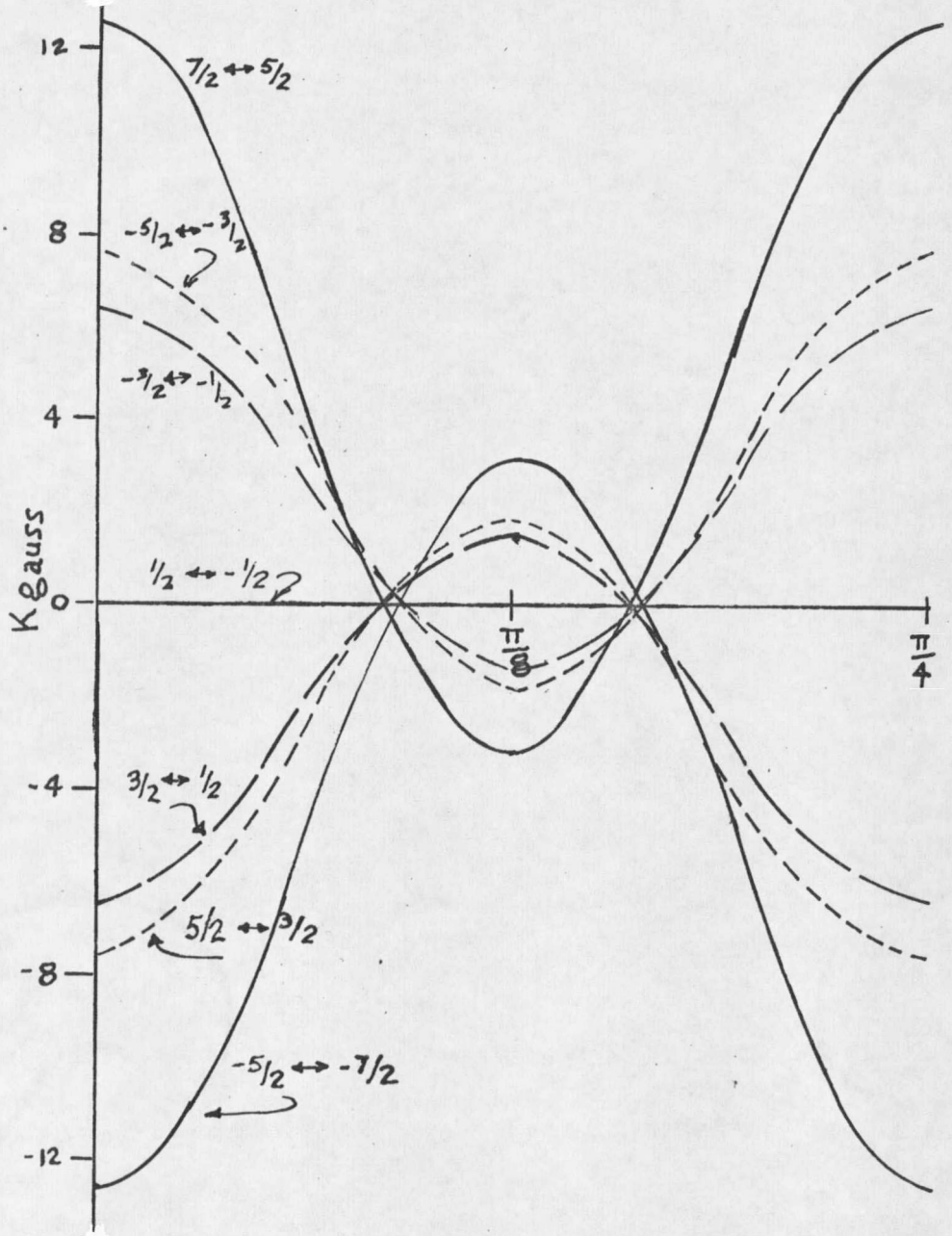

Figure 2.6 The angular dependence of the fine-structure spectrum rotated about a (100) axis.

CHAPTER III

THE E. P. R. EXPERIMENT AND THE HYPERFINE INTERACTION

Magnetic Resonance

The principle of magnetic resonance experiments is the Zeeman effect. In this experiment a gyromagnetic top is placed in a magnetic field. The interaction between the magnetic moment

$$\vec{\mu} = -\gamma\hbar\vec{J} \qquad 3.1$$

and the magnetic field causes a Larmor precession of the top. $\hbar\vec{J}$ is the angular momentum of the top. The torque on a magnetic moment $\vec{\mu}$ in a magnetic field is

$$\vec{T} = \vec{\mu} \times \vec{H}$$

From mechanics $\vec{T} = \frac{d\hbar\vec{J}}{dt}$, thus

$$\frac{d}{dt}\left[-\frac{1}{\gamma}\vec{\mu}\right] = \vec{\mu} \times \vec{H} \qquad 3.2$$

The solution to this equation, where $\vec{H}$ is constant and the angle between $\vec{\mu}$ and $\vec{H}$ nonzero, is a precession of frequency

$$\vec{\omega}_0 = \gamma\vec{H}_0 \ . \qquad 3.3$$

The energy levels of the paramagnets of eq. 3.2 are fixed, depending on the component of $\vec{\mu}$ in the direction of

$\vec{H}$.

$$\vec{E} = -\vec{\mu} \cdot \vec{H}. \qquad 3.4$$

If $\vec{H}$ is not a constant but is perturbed by a weaker magnetic field at right angles to $\vec{H}_0$, the perturbing field $\vec{H}_1$ will appear to average to zero from a reference frame rotating at the Larmor frequency. When $\vec{H}_1$ is also rotated, it will have an average life-time as an effective field when the rotation is close to the Larmor frequency. When the two frequencies are the same, resonance occurs giving rise to the name magnetic resonance. From the view of the rotating reference frame, when $\vec{H}_1$ is in resonance, the field $\vec{H}_0$ appears to be zero and $\vec{H}_1$ now will cause a precession of $\vec{\mu}$ about $\vec{H}_1$ changing the eigenstates of $\vec{J}$ to other combinations within the manifold of $2J + 1$. These transitions both absorb and emit energy to the system maintaining $\vec{H}_1$.

The coordinate system is selected such that z is along the magnetic field H_0 and the perturbing field is the magnetic component of sinusoidal microwave radiation. The Hamiltonian is

$$H = H_o + H_1 \qquad 3.5$$

where H_o is the spin Hamiltonian, which for the present discussion will be the electronic Zeeman term

$$H_0 = g\beta\vec{H}\cdot\vec{S} = g\beta H_0 S_z \qquad 3.6$$

in the representation of Chapter II.

$$H_1 = g\beta\vec{H}_1\cdot\vec{S} \qquad 3.7$$

and

$$\vec{H}_1 \rightarrow \vec{H}_1 \cos \omega t. \qquad 3.8$$

The probability per unit time that a paramagnet initially in state $|m>$ will be in state $|m'>$ from time dependent perturbation theory is

$$w_{mm'} = q^2\beta^2 H_1^2 |S_x^{mm'}|^2 g(\nu) \qquad 3.9$$

If the spin-lattice relaxation mechanism keeps an excess of the paramagnets in the lower energy states the distribution function $g(\nu)$ will be Loretzian,

$$g(\nu) = \frac{n\ 2T_2}{1 + T_2^2(2\pi)^2\ (\nu_0 - \nu)^2} \qquad 3.10$$

where T_2 is the characteristic spin-lattice relaxation time introduced into the Bloch equation (Pake, 1962).

In a sample with a large number of paramagnets, and given a time long compared to the relaxation times, the probable number of paramagnets at an energy $E_m = \vec{\mu}_m \cdot \vec{H}$ is governed by Boltzmann statistics,

$$\frac{N}{N_0} = \frac{e^{-E_m/kT}}{e^{-Em/kT}} \quad ; \quad -S \leq m \leq S \qquad 3.11$$

when

$$E_n << kT; \quad \frac{N_m}{N_0} = \frac{1 - g\beta H m/kT}{2S + 1} \quad . \qquad 3.12$$

Then

$$\frac{\Delta N}{N_0} = \frac{N + 1}{N_0} - \frac{N}{N_0} = \frac{-g\beta H}{2kT\ (S + 1)} \qquad 3.13$$

From eq. 3.9 the operator

$$S_x = \frac{1}{2}\ (S_+ + S_-) \qquad 3.14$$

requires selection rules $\Delta M = \pm 1$. That is the only transitions between energy levels differing by $|\Delta M| = 1$ will be stimulated by the microwave radiation. Since the lower states are more populous

$$\Delta N = N_0\ g\beta H/2(S + 1)kT, \qquad 3.15$$

more simulated absorption will occur than stimulated emission. If the microwave power is low enough to prevent saturation, the line shape of eq. 3.10 will occur. Saturation occurs when the radiation is intense enough to equally populate both levels. When this occurs the ratio between microwave power absorbed by the sample and power

available is not linearly related to the population of paramagnets occupying the energy levels. The intensity of a resonance line will be controlled by the matrix

$$\langle M' | S_x | M \rangle \ .$$

An accurate measure of the intensity will be the area under the curve $w_{MM'}$

$$I = g^2\beta^2 H_1^{\,2} | S_x^{MM'} |^2 \int_{-\infty}^{\infty} g(\nu)\, d\nu \ ,$$

$$I = [g\beta H_1 | S_x^{MM'} | \ ]^2 . \qquad 3.16$$

Figure 3.1 is an actual plot of the absorption of microwave power versus the magnetic field for Eu^{++} in CaF_2. The six large lines are the $\Delta M = 1/2 \leftrightarrow -1/2$ transition when a (100) crystal field axis is along H_0. The small satellite-lines adjacent to the six major lines are the mutual spin flip with fluorine nuclei discussed by Baker, Hayes, and O'Brien (1960). The overlap of these lines is virtually eliminated at very low temperatures since the more uniform local fields sharpen the line shape function $g(\nu)$. The existence of six lines depict the further splitting of the M = 1/2 and M = -1/2 levels by the

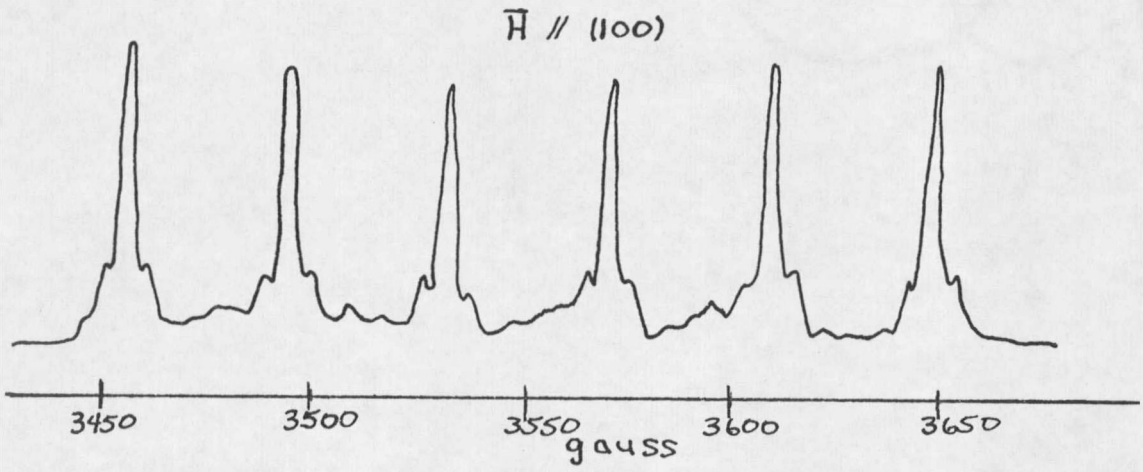

Figure 3.1

The direct absorption at X-band for $\Delta M = 1/2 \leftrightarrow -1/2$.

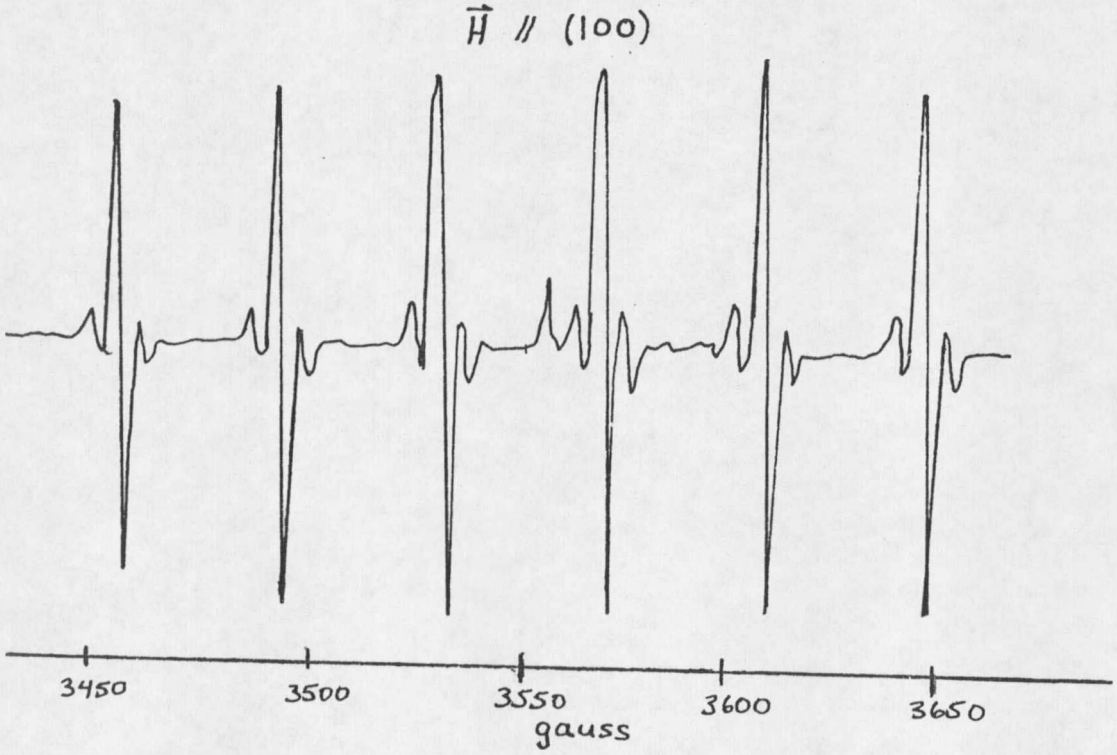

Figure 3.2

The phase detected $\Delta M = 1/2 \leftrightarrow -1/2$ absorption with field modulation.

hyperfine interaction, which will be explained later in this chapter.

The method for producing the microwave frequency magnetic field H_1 perpendicular to H_o and of detecting absorption is detailed in Appendix B. It is noted, however, that the spectrometer measures the derivative of the absorption lines not the lines of Fig. 3.1. Figure 3.2 is a display of the microwave absorption detected in this manner for the same $\Delta M = 1/2 \leftrightarrow -1/2$ spectrum.

The Hyperfine Splitting

The smallest energy splitting measured in the experiment was the hyperfine interaction. The Hamiltonian of an electron in a magnetic field $\vec{H}$, is derived from a vector potential. This discussion of the hyperfine interaction is well-treated by Milford, 1960, and is reproduced in Appendix D. Another spin Hamiltonian term is introduced into the phenomenological Hamiltonian of Chapter II

$$H(\text{Hyperfine}) = \vec{I} \cdot \vec{\vec{A}} \cdot \vec{S} \qquad 3.17$$

where $\vec{\vec{A}}$ is a symmetric tensor of order 2. For Eu impurities in fluorine crystals, $\vec{\vec{A}}$ is also isotropic and

$$H_{hf} = A \vec{I} \cdot \vec{S} \qquad 3.18$$

The spin Hamiltonian is now

$$H = g\beta\vec{H}\cdot\vec{S} + \frac{b_4}{60}(O_4^0 + 5O_4^4) + \frac{b_4}{1260}(O_6^0 - 21O_6^4)$$

$$+ A\vec{I}\cdot\vec{S} + g_n\beta_n\vec{I}\cdot\vec{H} \qquad 3.19$$

the last term being the nuclear Zeeman term.

For Eu the basis functions now included the nuclear function belonging to I^2 and I_z. Note, the nuclear spin I is 5/2 for both isotopes 151 and 153 which occur in abundance.

$$I = 5/2; \quad -5/2 \leq m \leq 5/2 \qquad 3.20$$

If a product wave function

$$\Psi = \Psi_e\Psi_n = |\gamma SM\rangle|Im\rangle$$

is used as a basis with respect to some common z axis, $\Psi = |M,m\rangle$ S and I implied, the matrix formed from H of eq. 3.10 and the $|M,m\rangle$'s having selected a coordinate system, would be an 8 x 6 = 48 matrix.

Calculation of Core Hyperfine Field

The 48 by 48 matrix can be diagonalized numerically for specific orientations of the crystal axes. The difficulty of this method can be reduced when the crystal field parameter is small relative to the Zeeman term.

Drumheller and Rubins (1964) have used perturbation theory to approximate the diagonalization when B_4 is very small.* For rather large B_4 such as is found in Eu^{++} in cubic crystals, this method may only be successful for very high external magnetic fields. It was found that a microwave frequency of 55 GHz was too great to allow clear resolution of forbidden transitions of Eu^{++} hyperfine lines in fluorite crystals. Perturbation techniques can be used to diagonalize the electronic 8 by 8 matrix when the wave functions of the spin Hamiltonian is written in a representation of the product of the eigenfunctions of I and S.

$$\Psi_{M,m} = \Psi^e_M \, \phi_m^{(M)} \quad . \qquad 3.21$$

For this purpose the Hamiltonian 3.19 is written as

$$H = H^e + H^n + H^{en} \qquad 3.22$$

where the electronic hamiltonian is

$$H^e = g\beta \vec{H} \cdot \vec{S} + \frac{b_4}{60} (O_4^0 + 5O_4^4) \qquad 3.23$$

In eq. 3.23 the order six terms of eq. 3.19 have been left off. The terms are small and need only be included when energy levels are being computed. The nuclear Hamiltonian

*b_4 about 1/2 when A is about 100×10^{-4} cm^{-1}.

having eigenfunctions $\phi_m^{(M)}$ is

$$H'_n = g_n \beta_n \vec{H} \cdot \vec{I}. \qquad 3.24$$

In eq. 3.24 quadrupolar terms are also left off. The term which couples the eigenfunctions of H^e and H^n is the hyperfine term

$$H^{en} = A\, \vec{I} \cdot \vec{S}\ . \qquad 3.25$$

It is because of the coupling term eq. 3.25 that the nuclear wave functions $\phi_m^{(M)}$ are written as dependent on the electronic state indexed M. The fine structure levels of Chapter II are the

$$E_M^e\ \delta_{MM'} = \langle \Psi_M{}^e | H^e | \Psi_{M'}{}^e \rangle \qquad 3.26$$

of eq. 2.19 with the angular correction of eq. 2.20 included. The $\Psi_M{}^e$'s are the functions which diagonalize H^e. Using the representation of eq. 3.21

$$\begin{aligned} &\langle \Psi'_{Mm} | H | \Psi_{M'm'} \rangle = E^e{}_M\ \delta_{MM'} \\ &+A \langle \Psi_M{}^e | \vec{S} | \Psi_{M'}{}^e \rangle \cdot \langle \phi_m^{(M)} | \vec{I} | \phi_{m'}^{(M)} \rangle \qquad 3.27 \\ &+g_n \beta_n \vec{H} \cdot \langle \phi_m^{(M)} | \vec{I} | \phi_m^{(M)} \rangle \phi_{mm'}\ . \end{aligned}$$

If A is small such that $A(E_M{}^e - E_M{}^e)$ is much less than one, it is possible to set M = M' in eq. 3.37 and not lose

accuracy in the hyperfine term.* Thus the spirit of the calculation implies accuracy to 1%. Then to find the eigenvalues of nuclear energy $E^{(M)}_m$ and the eigenfunctions $\phi_m^{(M)}$, the 2I + 1 matrix of H'_n must be diagonalized. The prime of H'_n refers to the dependence of the set $\{\phi_m^{(M)}\}$ on the electronic states.

The second term in eq. 3.27

$$H^n_{MM,m'm} = A\langle\Psi^e_M|\vec{S}|\Psi^e_{M'}\rangle \cdot \langle\phi_m^{(M)}|\vec{I}|\phi_{m'}^{(M)}\rangle \qquad 3.28$$

and the last term of eq. 3.27

$$H^n_{MM',m'm} = g_n\beta_n\vec{H} \cdot \langle\phi_m^{(M)}|\vec{I}|\phi_{m'}^{(M')}\rangle \qquad 3.29$$

can be combined to a single nuclear term where M = M'. Thus eqs. 3.28 and 3.29 become

$$\langle\phi_m^{(M)}|(g_n\beta_n\vec{H} + A\langle\Psi_M^e|\vec{S}|\Psi_M^e\rangle)\cdot\vec{I}|\phi_m^{(M)}\rangle.$$

The $\frac{A}{g_n\beta_n}\langle\Psi^e_M|\vec{S}|\Psi^e_M\rangle$ has units of magnetic field. It is termed variously as the "induced" field, the core hyperfine field and Bir's effective field after G. L. Bir (1964) who originally developed the theory. The "effective"

---

*For Eu^{++} in CaF_2, A = 34 x 10^{-4} cm^{-1} and $E^e_M - E^e_M$ is about 0.3 cm^{-1}.

field as seen by the nucleus then is

$$\vec{H}^{(m)}_{eff} = \frac{A}{g_n \beta_n} \langle \Psi^e_M | \vec{S} | \Psi^e_M \rangle . \quad (\vec{I}) \qquad 3.30$$

The field direction and magnitude depend on the electronic states Ψ_M which have an angular dependence in this representation on the crystal field orientation. Physically one views this field as being the magnetic field the nucleus sees because of the orbital electrons. The total field at the nucleus is $\vec{H}_j = \vec{H}_{eff} + \vec{H}_0$, the vector sum of the external field and the effective field. For A = 34×10^{-4} cm^{-1} and nuclear magneton $\beta_n = 5.03538 \times 10^{-24}$ μg/G and the spectroscopic splitting factor g_n is 1.44 for Eu^{151} and 0.637 for Eu^{153}, we have then $H_{eff} = 92{,}700\ \vec{S}_{M,M}$ gauss for Eu^{151} and $44{,}500\ \vec{S}_{M,M}$ gauss for Eu^{153}. When the experiment on Eu^{151} is done at X-band (ν = 10 GHz) the external magnetic field is about 3,600 gauss for the transitions M = 1/2 ↔ -1/2 which are of most importance to the experiment. Thus the external field is less than 4% of the induced field. In this case the induced field will dominate as the quantization axis of the nuclear Zeeman effect.

When an electronic transition occurs the effective field changes both magnitude and direction such as to

rotate the effective quantization axis $(\mathcal{H}_{eff}+\mathcal{H})/|\mathcal{H}_{eff}+\mathcal{H}| = z$. The eigenfunctions in the rotated system can be expressed as a linear combination of the set $\{\phi_m^{(M)}\}$ belonging to the manifold of I. The unitary transformation matrix which represents a rotation is

$$[T^I_{mm}(\alpha,\beta,\gamma)] = T$$

and transforms the set of orthonormal ϕ_m's as

$$\phi_m = \sum_{m'} T^I_{mm'}(\alpha,\beta,\gamma)\phi_{m'} \quad . \qquad 3.31$$

The specific form for this matrix $T^I_{mm'}$, is the operator

$$R_{\vec{u}}(\theta) = \exp[-i\theta\vec{J}\cdot\vec{u}] = e^{-i\gamma J_z}\, e^{-i\beta J_x}\, e^{-i\alpha J_z} \qquad 3.32$$

$\vec{u}$ is the unit vector defining the axis of rotation in 3-space, θ is the angle of rotation about the axis and $\vec{J}$ is the angular momentum operator. Expressing the arbitrary rotation in terms of Euler's angles, α is a rotation about the z axis, β a second rotation about the new x axis then γ a rotation about the z axis of the previous system. These three rotations can be made equivalent to a single rotation θ about $\vec{u}$ (Messiah, 1962). Gel'fand, Minlos, and Shapiro (1963) have found an expression for this matrix and expresses $e^{-\beta J_x}$ of eq. 3.32 as the matrix

$$R_x = R(\beta) = [P^I_{mm'}(\mu)] \qquad 3.33$$

where μ is the cosine of β, I indexes the manifold of the $2I + 1$ matrix.

The matrix of eq. 3.32, $e^{-i\gamma J_z}$ and $e^{-i\alpha J_z}$, can be shown to be simply

$$e^{-i\gamma J_z}|M\rangle = e^{-i\gamma M}|M\rangle \quad \text{(Messiah, 1962)} \qquad 3.34$$

The derivation of the matrix $[P_{mm}^{I}(\mu)]$ is shown in Appendix A. The nuclear eigenfunctions in the representation which has the quantization axis shifted by differing electron spin states then becomes

$$\phi_m^{(M)} = \sum_{M'} P_{mm}^{I}(\mu)\ \phi_m^{(M)} \quad . \qquad 3.35$$

In eq. 3.35 the function $\cos\theta = \mu$ depend on the angle between the electronic states M, M'.

$$= \cos(\vec{H}_M\ \vec{H}_{M'})$$

(see eq. 3.30). This dependence then accounts for the angular dependence of the hyperfine coupling; that is, while $P_{mm'}^{I}(\mu)$ is a rotation matrix in the space spanned by the nuclear eigenfunctions $\phi_m^{(M)}$, its argument depends on the electronic eigenfunction Ψ_m^e. Actually μ depends on the transition between the eigenfunctions Ψ_M^e.

From eq. 3.27 the energy eigenvalues are

$$E_m^{\mu} = E_e^{MM} + g_n\beta_n[\vec{H}_{eff} + \vec{H}] \cdot I \qquad 3.36$$

The effective field can be substituted for the total field in the nuclear Zeeman term, thus

$$E_n^M = g_n \beta_n m H_{eff}^{(M)} . \qquad 3.37$$

The field $H^{(M)}$ can be calculated from eq. 3.30 and becomes

$$\text{a) } H_x^{(M)} = \frac{A}{g_n \beta_n} \langle \Psi_M^e | \frac{S_+ + S_-}{2} | \Psi_M^e \rangle$$

$$\text{b) } H_y^{(M)} = \frac{A}{g_n \beta_n} \langle \Psi_M^e | \frac{S_+ - S_-}{2} | \Psi_M^e \rangle$$

$$\text{c) } H_z^m = \frac{A}{g_n \beta_n} \langle \Psi_M | S_z | \Psi_M^e \rangle . \qquad 3.38$$

From Chapter II when the crystal axes are rotated in the x-z plane by an angle θ, the electronic wave functions become

$$|\Psi_M^e\rangle = |M\rangle + \sum_{M'}{}' \frac{\langle M|V_1|M'\rangle}{E_M^0 - E_{M'}^0} |M'\rangle$$

$$+ \sum_k{}' \sum_\ell \left[\frac{\langle k|V_1|\ell\rangle\langle \ell|V_1|M\rangle}{(E_M^0 - E_k^0)(E_M^0 - E_\ell^0)} \right.$$

$$\left. + \frac{\langle M|V_1|M\rangle\langle k|V_1|M\rangle}{(E_M^0 - E_k^0)^2} \right] |k\rangle \qquad 3.39$$

where V_1 is the crystal field interaction of the fourth order spherical harmonics.

$$V_1 = \frac{b_4}{60}\{(\frac{3}{8} + \frac{5}{8}\cos 4\theta)O_4^0 + (\frac{5}{2} - \frac{5}{2}\cos 4\theta)O_4^2$$

$$+ (\frac{35}{8} + \frac{5}{8}\cos 4\theta)O_4^4 - 5i \sin 4\theta(O_4^1 - iO_4^2)\} \quad 3.40$$

The sixth order harmonics are not included because of the small value of b_6*. In eq. 3.39 the $|M,m>$'s are the $|M>$'s which are the eigenfunctions of S_z when the magnetic field is selected as the z direction.

In order to calculate the energy levels directly from perturbation theory the entire spin Hamiltonian of eq. 3.19 is used with product wave functions $|M,m>$ used as the representation. In this calculation the perturbation V_1 is the crystal field plus the hyperfine interaction. Again as in the induced field method the nuclear Zeeman term is left off. With the hyperfine term written as

$$H_{hf} = A\vec{I}\cdot\vec{S} = A\{I_zS_z\} + \frac{A}{2}(S_+I_- + S_-I_+), \quad 3.41$$

and the crystal field interaction as eq. 3.40, the energy levels are calculated from second order perturbation theory

$$E_{M,m} = E^0_{M,m} + \langle M,m|H_1|M,m\rangle + \sum_{M'm'}{}' \frac{|\langle M',m'|H_1|M,m\rangle|^2}{E^0_{Mm} - E^0_{M'm'}}$$

*$b_6 = 0.5\times10^{-4}$ cm^{-1}, $b_4 = 55\times10^{-4}$ cm^{-1} or b_6/b_4 0.99%.

With $H_1 + H_{eff} + H_{hf}$ from eqs. 3.40 and 3.41 the energy levels of eq. 2.16, M, m levels become,

a) $$E_{\pm 7/2,m} = \pm\frac{7}{2} g\beta H + \frac{7}{8} b_4(3 + 5\cos\theta) + b_6 \pm \frac{7}{2} Am + \frac{35}{4}\frac{b_4^2}{g\beta H_0} \pm \frac{A}{4g\beta H_0} 7\left(\frac{35}{4} - m^2 \pm m\right)$$

b) $$E_{\pm 5/2,m} = \pm\frac{5}{2} g\beta H - \frac{13}{8} b_4(3 + 5\cos\theta) - 5b_6 \pm \frac{5}{2} Am + \frac{75}{4}\frac{b_4^2}{g\beta H_0}\left[5\left(\frac{35}{4} - m^2\right) \pm 19\, m\right]$$

c) $$E_{\pm 3/2,m} = \pm\frac{3}{2} g\beta H - \frac{3}{8} b_4(3 + 5\cos 4\theta) + 9b_6 \pm \frac{75b_4^2}{4g\beta H_0} + \frac{3}{2} Am \pm \frac{A^2}{4g\beta H}\left[3\left(\frac{35}{4} - m^2\right) \pm 27\, m\right]$$

d) $$E_{\pm 1/2} = \pm\frac{1}{2} g\beta H + \frac{9}{8} b_4(3 + 5\cos 4\theta) - 5b_6 \pm \frac{35b_4^2}{4g\beta H} \pm \frac{1}{2} Am \pm \frac{A^2}{4g\beta H_0}\left[\frac{35}{4} - m^2 \pm 31\, m\right] \qquad 3.42$$

In the above expressions terms of order $\frac{b_4 b_6}{g\beta H}$, $\frac{b_6^2}{g\beta H}$ and $\frac{b_4^2}{g\beta H}\sin^2 4\theta$ are not included in the second order calculation. The above energy levels are accurate to the order of perturbation for $\theta \leq 5°$ which is adequate for the measurements discussed in Chapter IV.

In the E.P.R. experiment the energy of the photon

exciting transitions between the levels of eq. 3.42 is fixed and the resonance condition is achieved by varying the external field H_0. For the hyperfine transition, excluding a perturbation equal to or higher than $\Delta M = \pm 2$, the field where the transition occurs is called the line position. These transitions are;

$$\text{a) } \bar{H}^{mm'}_{\pm 7/2,\pm 5/2} = H_0 \pm 20b_4q \pm 6b_4 - \frac{1}{4H_0}[35(b_4q-3b_6)^2 - 3(5b_4q+7_b6)^2 - \frac{A}{2}(7m-5m') - \frac{A^2}{4H_0} \times\{7(\frac{35}{4} - m^2) - 5(\frac{35}{4} - m'^2) \pm (7m-19m')\}$$

$$\text{b) } \bar{H}^{mm'}_{\pm 5/2,\pm 3/2} = H_0 \pm b_4q \pm 14b_6 - \frac{A}{2}(5m-3m') - \frac{A^2}{4H_0} \times\{5(\frac{35}{4}-m^2) - 3(\frac{35}{4}-m'^2) \pm (19m-27m')\}$$

$$\text{c) } \bar{H}^{mm'}_{\pm 3/2,\pm 1/2} = H_0 \pm 12b_4q \pm 14b_6 - \frac{1}{4H_0}[3(5b_4q\pm 7b_6)^2 - 35(b_4q-3b_6)^2] - \frac{A}{2}(3m - m') - \frac{A^2}{4H_0} \times[3(\frac{35}{4} - m^2) - \frac{35}{4} + m'^2 \pm (27m-31m')]$$

$$\text{d) } \bar{H}^{mm'}_{\pm 1/2,\pm 1/2} = H_0 - \frac{35}{2_0}(b_6q-3b_6)^2 - \frac{A}{2}(m+m') - \frac{A^2}{4H_0} \times[\frac{35}{4} - m^2 - m'^2 \pm 31(m - m')] \quad . \qquad 3.43$$

In the above expressions terms of order b_6b_4/H and $(b)^2/H$

were dropped. Also a small angle was assumed such that the term of order $(b_4)^2/\mathcal{H}$ $\sin^2 4\theta$ were not included. $q = 1/8(3 + 5\cos\theta)$ determines the angular dependence for angles $\theta \leq 5°$. The allowed transitions of eq. 3.43 are displayed as the derivative of the microwave absorption versus the applied magnetic field. In the display of Fig. 3.2, the angle ϕ is zero. Figure 3.2 is the differentiated spectrum. Figures 3.3(a) through (c), show the transitions of Figure 3.2 as the angle θ is varied from zero to five degrees. It can be noticed that the line intensities are a function of angle, some lines being of zero intensity at zero degrees.

The transitions between the energy levels occur when the intensity, eq. 3.16, is other than zero.

$$I = g^2\beta^2\mathcal{H}_1^2|\langle M'm'|S_x|Mm\rangle|^2 \qquad 3.44$$

The operator $S_x = \frac{1}{2}(S_+ + S_-)$ induces transition which follow the selection rules $\Delta M = \pm 1$. The selection rules are with respect to the unperturbed eigenfunctions of S^2, S_z. If the wave functions of the energy levels were also eigenfunctions of S^2, S_z; the quantum numbers S and M would be said to be "good" quantum numbers. The wave functions are expressed as a linear combination of the

eigenfunctions of S^2, S_z; therefore, transitions between levels indexed M' and M of eq. 3.45 occur when M' and M do not differ by one. These transitions are usually weaker than those transitions between M, M' levels differing by one and are called "forbidden" transitions. In the Eu ion in fluorite crystals, "forbidden" transitions occur between levels indexed by different m as well, and are termed "forbidden hyperfine" transitions. As can be seen in Fig. 3.3, the forbidden lines can have greater intensity than allowed lines.

In the induced field method, the wave functions M, m are written in a representation where the product of wave function belonging to H_e and those belonging to H_n. The wave functions of H_n depend on the electronic state through the rotation matrix of eq. 3.35. Then eq. 3.45 becomes

$$I = q^2\beta^2H_1^2|\langle\Psi_e^{M'}\ \phi_m^{(M)}|S_x|\Psi_e^{M}\ \phi_{m'}^{(M)}\rangle|^2$$

$$g^2\beta^2H_1^2|\langle\Psi_e^{M}|S_x|\Psi_e^{M}\rangle|^2\ |\langle\phi_m^{M}|\phi_{m'}^{M}\rangle|^2 \qquad 3.45$$

Note that this expression consists of two parts, the probability of an electronic transition

$$w_n^{mm'} = |\langle\phi_m^{M}|\phi_{m'}^{M}\rangle|^2. \qquad 3.46$$

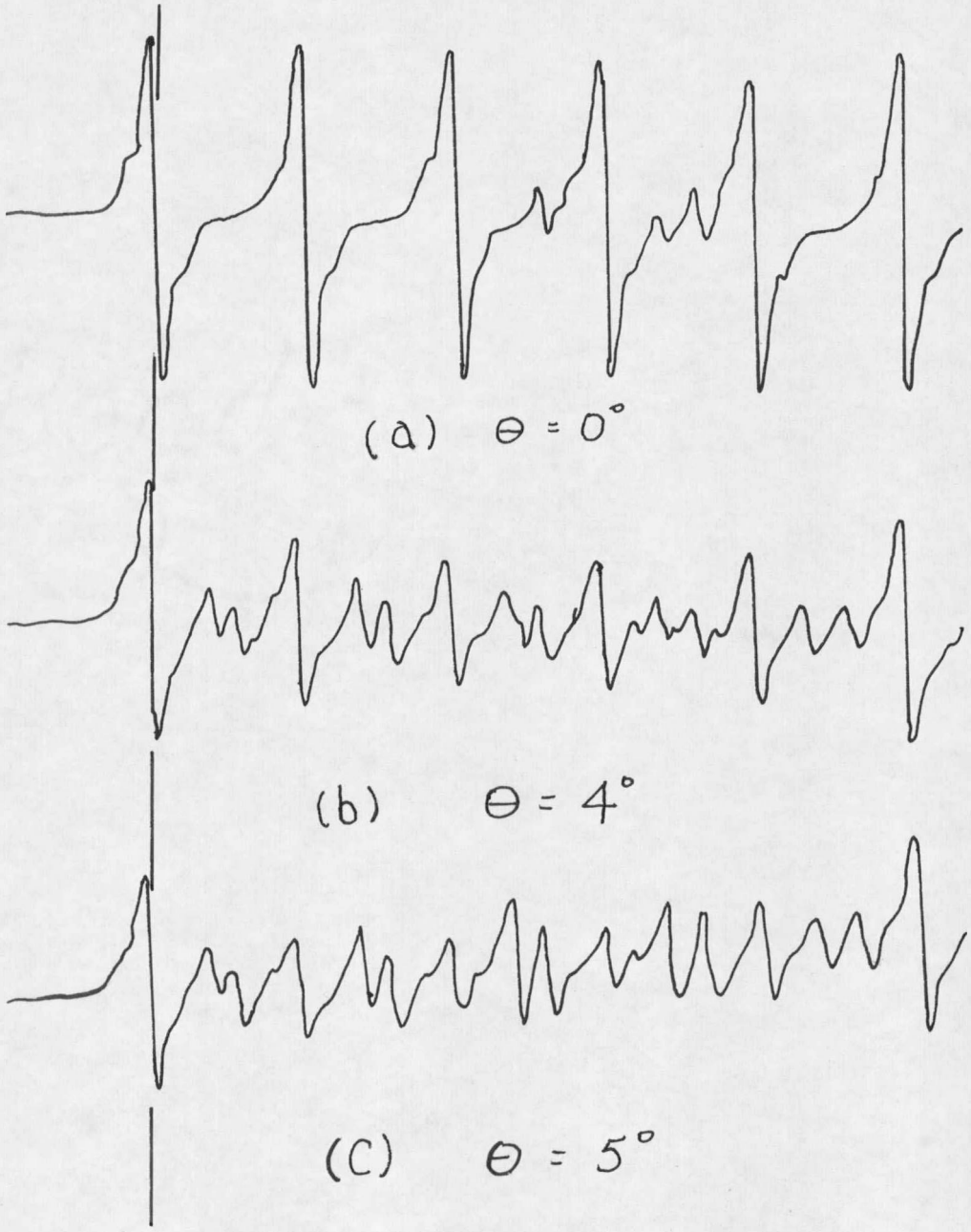

Figure 3.3 Hyperfine spectrum for $\Delta M = 1/2 \leftrightarrow -1/2$. Taken at room temperature, compare line width with Fig. 3.2. θ is angle between field and (100) axis.

Substituting from eq. 3.42, 3.46 becomes

$$w_n^{mm'} = |\langle \phi_m^M | \sum_{m'} P^I_{mm'}(\mu) | \phi_{m'}^M \rangle|^2 . \qquad 3.47$$

In eq. 3.47 the superscript M's are now the same, the set $\{\phi_m^M\}$ is an orthonormal set thus

$$w_n^{mm'} = |P^I_{mm'}(\mu)|^2 \qquad 3.48$$

The line intensities of eq. 3.45 can be found using $P^{5/2}_{mm'}(\mu)$ matrix elements of Table 3.2 (see Appendix A).

Table 3.2

Analytic Form of the Functions $|P_{mm'}(\mu)|^2$

(Bir and Sochava, 1964)

$\lvert P_{5/2,5/2}\rvert$	$\lvert P_{3/2,3/2}\rvert$	$\lvert P_{1/2,1/2}\rvert$	$\lvert P_{5/2,3/2}\rvert$
$(\frac{1+\mu}{2})^5$	$(\frac{1+\mu}{2})^3 \cdot (\frac{3-5\mu}{2})^2$	$(\frac{1+\mu}{2}) \cdot (\frac{5\mu^2-2\mu-1}{2})^2$	$5 \cdot (\frac{1-\mu}{2}) \cdot (\frac{1+\mu}{2})^4$

$P_{3/2,1/2}$	$P_{5/2,1/2}$
$(\frac{1+\mu}{2})^2 \cdot (1-\mu) \cdot (\frac{1-5\mu}{2})^2$	$10(\frac{1-\mu}{2})^2 \cdot (\frac{1+\mu}{2})^3$

The argument of the $P^{I}_{mm'}(\mu)$'s, μ, is the cosine of the angle between the core hyperfine fields of state M and M'. The indeces M and M' are those of the corresponding electronic part of the intensities of eq. 3.45. The experiment to be described in Chapter IV was performed by rotations of θ about a (100) crystal axis, thus by choice, the rotations take place in the x-z plane.

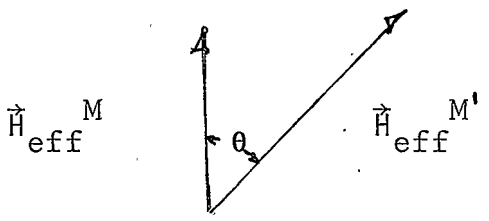

Figure 3.4

$$\mu = \cos\theta = \frac{H_{eff}^{M} \cdot H_{eff}^{M'}}{|H_{eff}^{M}||H_{eff}^{M'}|} . \qquad 3.49$$

$$\mu = \frac{H_z^{M} H_z^{M'} + H_x^{M} H_x^{M'}}{\sqrt{H_z^{(M)2} + H_x^{(M)2}}\sqrt{H_z^{(M')2} + H_x^{(M')2}}} \qquad 3.50$$

$$(H_z^2 + H_x^2)^{-1/2} = H_z^{-1}\left[1 + \left(\frac{H_x}{H_z}\right)^2\right]^{-1/2} \qquad 3.51$$

when H_x/H_z is small a Taylor's expansion of eq. 3.51 sub-

stituted into eq. 3.50 results in

$$\mu = \frac{H_z^{M'} H_z^{M}}{|H_z^{M} H_z^{M'}|} \{1 - \frac{1}{2}[\frac{H_x^{M}}{H_z^{M}} - \frac{H_x^{M'}}{H_z^{M'}}] + \ldots\} \qquad 3.52$$

Substituting eq. 3.38 into 3.52 and using Ψ_e^M to first order, only 0_4^1 is present in the perturbation calculation of H_x^M. In the calculation, a symmetrized S_x times 0_4^1 results in an 0_4^0 and 0_4^2 combination.

$$S_{\pm} Y_4^{\pm 1} = \sqrt{S(S+1) - M(M\pm 1)}\ Y_4^{2,0,-2}$$

Then eq. 3.52 becomes

$$\mu = \frac{MM'}{|MM'|}[1 - \frac{1}{2}(\frac{b_4 \sin 4\theta}{24 g\beta H})^2 (\frac{\langle M|0^0_4|M\rangle}{M} - \frac{\langle M'|0^0_4|M'\rangle}{M'})] \qquad 3.53$$

The values of the matrix elements of 0^0_4 are found in Low (1960, page 18). The approximation of eq. 3.53 is accurate for angles less than 10°. For angles greater than 10°, higher order calculations of eq. 3.50 could be made using Ψ_e^M calculated to higher orders.

Eq. 3.53 is greater for the $\Delta M = 1/2 \leftrightarrow -1/2$ electronic calculation. The intensities of the lines in this group, therefore vary greatly as is seen from Fig. 3.3. Bir, Butikov, and Sochara (1965) measuring intensities of the $\Delta M = 1/2 \leftrightarrow -1/2$ spectrum were able to verify the predicted

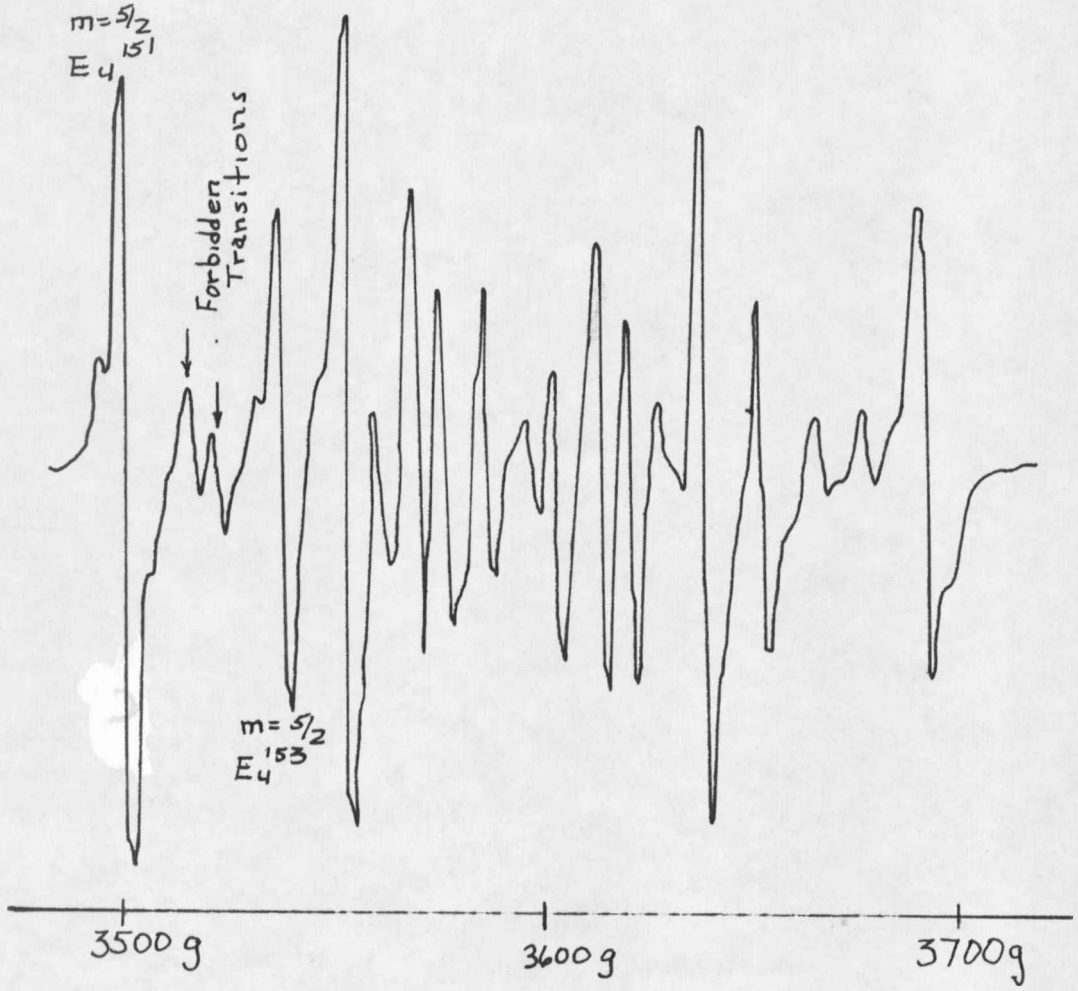

Figure 3.6 The $\Delta M = 1/2 \leftrightarrow -1/2$ hyperfine spectrum with both isotopes Eu^{151} and Eu^{153} in CaF_2. The magnetic field is 3° to a (100) axis.

intensities of this theory for some lines of the spectrum. Namely the allowed $\Delta m = \pm 5/2 \leftrightarrow \pm 5/2$ $\Delta m = \pm 3/2 \leftrightarrow \pm 3/2$ transitions and the forbidden $\Delta m = \pm 5/2 \leftrightarrow \pm 3/2$ and $\Delta m = \pm 5/2 \leftrightarrow \pm 1/2$ transitions. Application of the theory to other lines was not attempted because they used an europium sample containing both isotopes 151 and 153. Figure 3.6 shows the confusion resulting in this case since the two isotopes have different hyperfine coupling constants. Stice and Worsencroft (1970) were able to verify the theory for other lines in the $\Delta M = 1/2 \leftrightarrow -1/2$ spectrum by using the single isotope Eu^{151}. In that same work the weaker forbidden lines $\Delta m = \pm 1$ in $\Delta M = \pm 3/2 \leftrightarrow \pm 1/2$ spectrum were found and the theory applied to show good agreement. This was the first report of these lines as far as the author was able to ascertain. Figure 3.7 is a display of the $\Delta M = 3/2 \leftrightarrow 5/2$ spectrum which overlaps the $\Delta M = \frac{5}{2} \leftrightarrow \frac{3}{2}$ spectrum. In Fig. 3.7 the same spectrum is displayed when an angle of 2 1/2° was between the magnetic field and a (100) crystal axis. Figure 3.7(b) is a histogram of the position of the expected energy from the theory, the height is relative to the expected intensity and the width the measured line with at 78°K from the experiment.

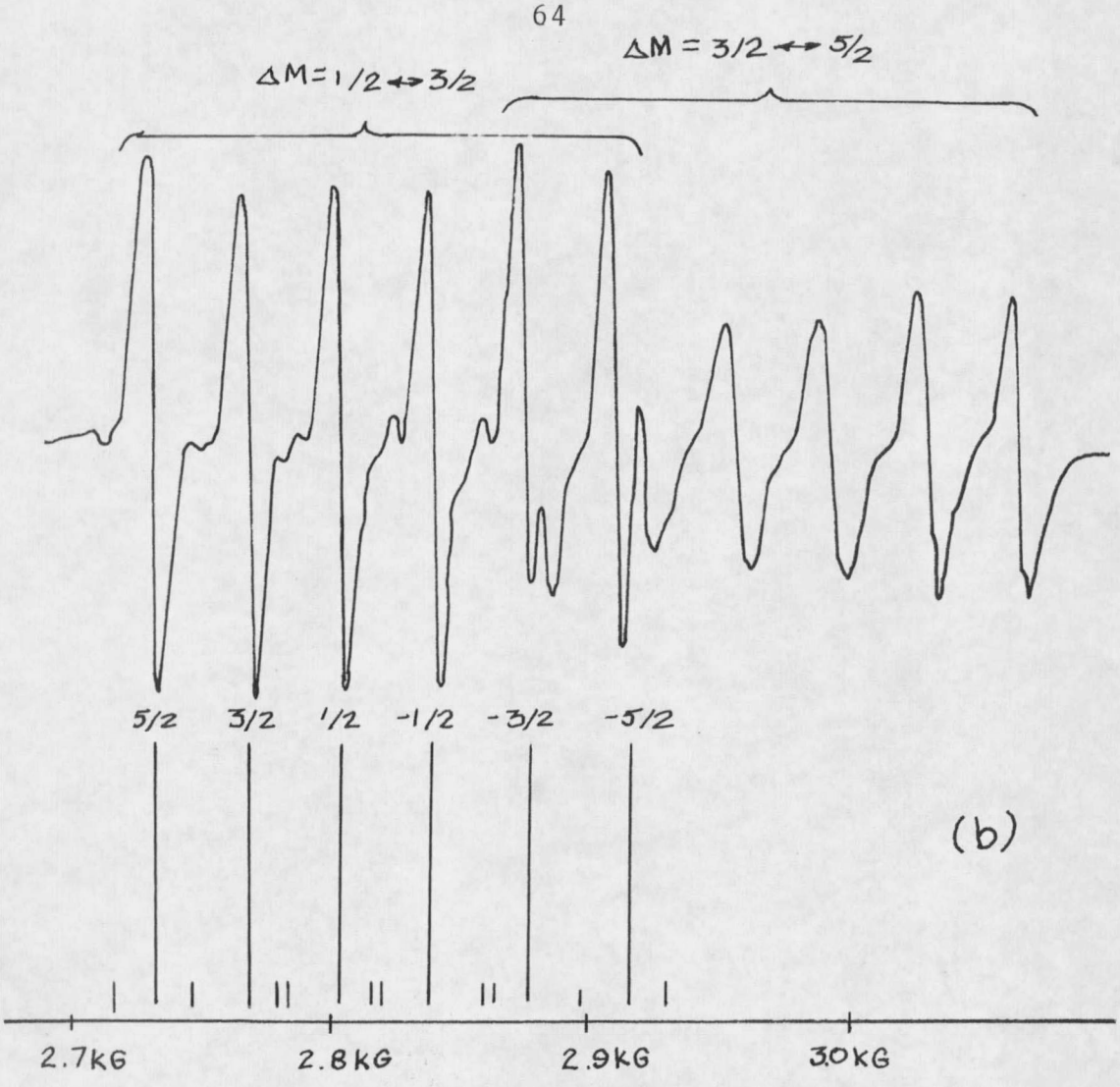

Figure 3.7 Forbidden hyperfine lines in the $\Delta M = 3/2 \leftrightarrow 1/2$ spectrum of Eu-CaF_2. The doublet between M = 1/2, and M = -1/2 was later resolved but that between M = -1/2 and M = 3/2 was not.

Table 3.3

The line positions calculated for the hyperfine spectrum of Figure 3.7.

H_{center} = 3547 - 726 = 2823 gauss, the lines from left to right of the M = 1/2 3/2 are:

5/2,3/2 = H_c-108.3	1/2, 1/2 = H_c-19.7	-5/2,-3/2 = H_c+108
5/2,5/2 = H_c-91.4	1/2,-1/2 = H_c-41.1	-3/2,-5/2 = H_c+38.6
3/2,5/2 = H_c-38.7	-1/2, 1/2 = H_c+41.4	-3/2,-3/2 = H_c+54
3/2,1/2 = H_c-76.9	-1/2,-3/2 = H_c-5.0	-5/2,-5/2 = H_c+91
1/2,3/2 = H_c- 1.3	-3/2,-1/2 = H_c+75.3	
3/2,3/2 = H_c-55.5	-1/2,-1/2 = H_c+15.6	

CHAPTER IV

ORBIT-LATTICE INTERACTION

Necessary Approximations

Chapter II dealt with the interaction of the paramagnetic electrons and the crystal field. Chapter III then presented a theory which predicted the intensities of the E.P.R. transitions as function of spatial orientation. Both presentations assumed the crystal-lattice to be rigid. That is, the position of the lattice sites were assumed to be fixed in time. There is, of course, an internal energy which is associated with the vibrational-kinetic motion of the ions. Several macroscopic phenomena can be explained from the quantum treatment of these vibrations, called lattice vibrations. The local surroundings of the paramagnetic ions in fluorite crystals is altered in such a way as to "couple" the quantized vibrations or phonons to the paramagnetic electrons. Thus, temperature changes will shift the energy levels and subsequently alter the E.P.R. spectrum as to line position as well as the intensity of the hyperfine spectrum.

In this chapter appropriate corrections to the crystal field parameters will be proposed by an analysis of

of the orbit-lattice interaction. This interaction can be imagined to be an interaction between the quantized lattice vibrations and the paramagnetic electrons.

The potential energy term or binding energy of a periodic crystal varies as the ions in the crystal are displaced from equilibrium by a displacement $\vec{u}_{s\ell}$ of the sth ion in the ℓth unit cell. The potential expanded in a Taylor's series is

$$V = V_0 + \sum_{s\ell j} u_s{}^j{}_\ell \left(\frac{\partial V}{\partial u_s{}^j{}_\ell}\right)_0 + \sum_{ss',\ell\ell',jj'} u_s{}^j{}_\ell \times u_{s'}{}^{j'}{}_{\ell'} \left(\frac{\partial^2 V}{\partial u_s{}^j{}_\ell \partial u_{s'}{}^{j'}{}_{\ell'}}\right)_0 + \sum_{ss's'',\ell\ell'\ell'',jj'j''} u_s{}^j{}_\ell u_{s'}{}^{j'}{}_{\ell'} u_{s''}{}^{j''}{}_{\ell''} \left(\frac{\partial^3 V}{\partial u_s{}^j{}_\ell \partial u_{s'}{}^{j'}{}_{\ell'} \partial u_{s''}{}^{j''}{}_{\ell''}}\right)_0 + \ldots \qquad 4.1$$

where $u_s{}^j{}_\ell$ refers to the jth cartesian component of $u_{s\ell}$. The cubic term in the binding energy expansion is the anharmonic term and it accounts for the first order correction to lattice expansion which would be zero if only harmonic corrections were considered. The effect of

anharmonic forces as explained by Ziman (1965) follows:

> "As the temperature rises the amplitude of the lattice vibrations increases, so that the average R.M.S. values of the displacement $u_{s\ell}$ etc., increase. The anharmonic terms contribute to the free energy of the crystal, which is now no longer necessarily a minimum for vibrations around the assumed 'equilibrium' configuration in which each $u_{s\ell}$ vanishes. The whole crystal then expands (or contracts) until it finds the volume where the total free energy is a minimum."

In analyzing the temperature dependence, corrections for lattice expansion will be made as if it were an independent effect from the harmonic term. This assumption, that the effects can be separated, is then based on the assumption that a Taylor's series expansion is valid.

In Chapter V corrections for the anharmonic term will be made from measurements of the dependence of crystal-field parameters on hydrostatic pressure. Then the crystal field will be expanded as a Taylor's series in terms of the ion displacements. As a further simplification it is assumed that only nearest neighbor ions will contribute to a crystal field, thus upon replacing the displacement variables with normal mode variables only the 27 normal modes of the XY_8 functional cell will be considered. The normal modes will then be written in terms of phonons by quantizing the harmonic oscillators and a simple Debye model will allow

averaging which will predict a temperature dependence.

To effect these corrections a model based on vibrations of small amplitude is adopted. The binding energy of the crystal, which is assumed to be a function of the positions of the ions, is expanded in a Taylor's series of displacements from equilibrium of the ions. The equilibrium state is that where no unbalanced force would be acting on the ions. The expression to third order terms is eq. 4.1. The zero order term is constant and can be neglected as long as the crystal remains intact. The first order term is zero from the definition of equilibrium. The quadratic order term is called the harmonic term and approximates the deviation from a rigid lattice by considering a restoring force which varies linearly with displacement. The harmonic motion of the ions will affect the crystal-field seen by the paramagnetic ions. The crystal-field should not be confused with the binding energy of the crystal. The crystal-field is measured at the electron of a paramagnetic ion from a coordinate system fixed to the nucleus of that ion and is given in a simplified system which only considers the effect from the nearest neighbor fluorine ions.

Again, as in Chapter II, the classical solution of the

electric potential energy of the paramagnetic f electrons of Eu interacting with the eight ligand fluorine ions which are the nearest neighbors is expressed in terms of spherical harmonics

$$V_c = \sum_e \sum_{\ell=0}^{\infty} \sum_{m=\ell}^{\ell} r_e^{\ell} V_{\ell}^{m} Y_{\ell}^{-m} (\theta_e \phi_e). \qquad 4.2$$

In eq. 4.2 $\sum_e$ means the summation over all f electrons each being positioned at coordinates (r_e, θ_e, ϕ_e). Further simplification is obtained by assuming point charges for the fluorine ions. This assumption neglects covalency and overlap which, while they are not neglegable, are at least a lesser effect for deep-seated f electrons than would appear in transition metal ions (Simanek and Huang, 1966). Assuming point charges in eq. 4.2 the coefficients

$$V_{\ell}^{m} = \sum_{i=1}^{8} \frac{-e'e}{R_i^{\ell+1}} \frac{Y_{\ell}^{m}(\Theta_i \phi_i)}{2\ell+1} \qquad 4.3$$

where the ith fluorine ion is located at position (R_i, θ_i, ϕ_i) and has an effective charge e'. This potential energy results from a solution to the point charge LaPlace equation solved in terms of Legendre polynomials subsequently expanded to the solution of eq. 4.2 and 4.3 by the addition theorem for spherical harmonics (Arfkens, 1966).

The position of the fluorine ions (R_i,θ_i,ϕ_i) of eq. 4.3 is not constant. Because of lattice vibration, which are assumed to be much smaller in magnitude than R_i, V_c of eq. 4.2 can be expressed as a Taylor's series in terms of the cartesian coordinates of the ionic displacements α_j.

$$V_c = \sum_{\ell} \sum_{m=-\ell}^{\ell} \{V_\ell^m|_0 + \sum_{j,i} \frac{\partial V_\ell^m}{\partial \alpha_j^i})_0 \alpha_j^i + \ldots\}$$

$$x\ r_e^\ell Y_\ell^m (\theta_e,\phi_e) \qquad 4.4$$

In eq. 4.4 α_j^i refers to the α_j th component [α_j = (x,y,z) as j = (1,2,3)] of the displacement of the i ion. In the XY_8 functional cell there are 27 degrees of freedom; that is, the motion of the complex can be described with 27 linearly independent variables. The choice of the cartesian (x,y,z) components of all nine ions could be exchanged for "normal" coordinates of like number 27. The subscript 0 of eq. 4.4 refers to the value of these functions at zero displacement or at R_{io}, the equilibrium position. The first term of eq. 4.4 is then the rigid lattice crystal field presented in Chapter II. The term linear in α_j^i is called the orbit-lattice interaction following Van Vleck (1939).

The orbit-lattice interaction